Protist 174 (2023) 125965
http://www.elsevier.de/protis
Published online date 9 May 2023

Protist

Original Paper

Diverse eukaryotic phytoplankton from around the Marquesas Islands documented by combined microscopy and molecular techniques

Jana Veselá-Strejcová [a], Eleonora Scalco [b], Adriana Zingone [b], Sébastien Colin [c], Luigi Caputi [b], Diana Sarno [b], Jana Nebesářová [a], Chris Bowler [b,d] and Julius Lukeš [a,e,*]

[a]Institute of Parasitology, Biology Centre, Czech Academy of Sciences, 37005 České Budějovice (Budweis), Czech Republic
[b]Stazione Zoologica Anton Dohrn, Villa Comunale, 80121 Naples, Italy
[c]Max Planck Institute for Developmental Biology, 72076 Tuebingen, Germany
[d]Institut de Biologie de l'École Normale Supérieure, CNRS, INSERM, PSL Université Paris, 75005 Paris, France
[e]Faculty of Science, University of South Bohemia, 37005 České Budějovice (Budweis), Czech Republic

Submitted December 20, 2022; Accepted May 2, 2023
Monitoring Editor: Laure Guillou

Abstract

Oceanic phytoplankton serve as a base for the food webs within the largest planetary ecosystem. Despite this, surprisingly little is known about species composition, function and ecology of phytoplankton communities, especially for vast areas of the open ocean. In this study we focus on the marine phytoplankton microflora from the vicinity of the Marquesas Islands in the Southern Pacific Ocean collected during the *Tara* Oceans expedition. Multiple samples from four sites and two depths were studied in detail using light microscopy, scanning electron microscopy, and automated confocal laser scanning microscopy. In total 289 taxa were identified, with Dinophyceae and Bacillariophyceae contributing 60% and 32% of taxa, respectively, to phytoplankton community composition. Notwithstanding, a large number of cells could not be assigned to any known species. Coccolithophores and other flagellates together contributed less than 8% to the species list. Observed cell densities were generally low, but at sites of high autotrophic biomass, diatoms reached the highest cell densities (1.26×10^4 cells L^{-1}). Overall, 18S rRNA metabarcode-based community compositions matched microscopy-based estimates, particularly for the main diatom taxa, indicating consistency and complementarity

* Corresponding author.
e-mail: jula@paru.cas.cz (J. Lukeš).

https://doi.org/10.1016/j.protis.2023.125965

between different methods, while the wide range of microscopy-based methods permitted several unknown and poorly studied taxa to be revealed and identified.

Key words: diatoms; dinoflagellates; phytoplankton; marine protists; equatorial Pacific; *Tara* Oceans.

Introduction

The world's ocean covers more than 70% of the Earth's surface and is by far the largest ecosystem on our planet. Yet there is still a substantial lack of knowledge about its functional components, which is especially true for oceanic phytoplankton. Regardless of their very small size, these organisms play crucial roles as the base of oceanic food webs and in the regulation of global biogeochemical, ecological and climatic processes (Bowler 2013; Worden et al. 2015; Abreu et al. 2022). According to some estimates, marine phytoplankton are responsible for about 50% of global primary production, namely the generation of oxygen and fixation of atmospheric carbon, and thus represent a major component of the biological carbon pump (Field et al. 1998, Ducklow et al., 2001; Sigman & Hain 2012).

Studying such a vast and complex ecosystem is challenging for a range of reasons, including financial and logistical. Consequently, surveys of marine phytoplankton biodiversity tend to be either non-standardized, geographically restricted and/or do not consider the complete size spectrum of planktonic organisms (Caron et al. 2012). The 2009–2013 *Tara* Oceans campaign was one of the first to carry out a comprehensive worldwide sampling collection with a coherent strategy to record additional contextual data to permit a holistic study of the vast oceanic plankton ecosystem (Karsenti et al. 2011). During the four year expedition, thousands of samples along with numerous environmental measurements from 160 stations across the tropical and temperate oceans were collected, and were subsequently supplemented with 50 stations sampled during a Polar Circle circumnavigation (Pesant et al. 2015; Sunagawa et al. 2020).

Such a unique, global collection of over 40,000 samples promises to provide a comprehensive view of the planetary oceanic ecosystem (Sunagawa et al. 2020). It also allows a range of specific phenomena to be explored more deeply. One such example is the high primary productivity that has been observed perennially in the ultraoligo- to oligotrophic waters in the vicinity of the Marquesas Islands. This remote French Polynesian archipelago is located in the central equatorial Pacific, with its individual islands (10–25 km wide) rising steeply from the abyssal plain at a depth of 4 km. The islands are separated by 40 to 100 km wide channels, through which the strong South Equatorial Current flows westward past the islands (Legeckis, 1977). The origin of this prominent phytoplankton bloom, noted already in the 1960's and visible by ocean colour observations from space, was studied by Signorini et al. (1999) and Martinez & Maamaatuaiahutapu (2004), who proposed that it may be caused by an island mass effect. This effect, apparently an important contributor to the productivity in the area, is formed by a combination of factors, such as turbulent mixing and advection from the South Equatorial Current, iron-enriched waters originating from land drainage, and hydrothermal fluxes through old volcanic formations (Signorini et al. 1999).

The response of marine plankton communities to iron limitation and resupply in this area has been studied in great detail at four *Tara* Oceans stations (Caputi et al. 2019). This complex study of the mass effect of the islands in a stable ocean current focused mainly on the characterization of the ecological, ontological and transcriptomic responses of the plankton assemblages to iron, the key limiting micronutrient in the area. While millions of environmental sequences of genetic markers were obtained, most of them did not match with taxa available in public reference databases and could not be assigned to known species, while pigment composition only allowed taxonomic resolution at the higher taxonomic group level, e.g., phylum or order. On the other hand, microscopic techniques can provide a wealth of otherwise missing information concerning the diversity and distribution of planktonic organisms, which is sparse for remote oceanic regions such as the subequatorial central Pacific.

In this study we conducted a thorough taxonomic assessment of marine phytoplankton in the Marquesas region of the equatorial Pacific by applying light, electron, and confocal laser scanning microscopy techniques to different samples collected in August

2011. The aim of our investigation was to complement the study by Caputi et al. (2019) with detailed taxonomic information on the phytoplankton taxa found in this chronically understudied region. Furthermore, a comparison between the metabarcoding and morphological data was performed to highlight advantages and limitations of these different approaches.

Materials and methods

Study area

Phytoplankton samples collected during the *Tara* Oceans expedition in August 2011 from four sites surrounding the Marquesas Islands (Fig. 1; Table 1) were examined in this study. The first location (station TARA_122), situated approximately 30 km east of the islands, represented a control station, unaffected by the island mass effect. The following two stations (TARA_123, TARA_124) were located in the area with the highest phytoplankton densities, while the last one (TARA_125) was sampled approximately 250 km west of the islands, towards the periphery of the phytoplankton bloom (Fig. 1).

Hydrographic features and satellite images of the area under investigation were presented in Caputi et al. (2019) along with a metabarcoding-based overview of the main planktonic groups in various size fractions, in relation with their responses to different iron availability conditions. Here, we summarize some general features of the area in order to better characterize the environmental and biological contexts of our results. Chlorophyll *a* (Chl-*a*) values integrated over the water column varied among the sampled stations. Low concentrations (16.6 mg m^{-2}) coupled with relatively high nutrient levels were recorded at TARA_122, with conditions typical for a High Nutrient Low Chlorophyll Region (Quéguiner 2013; Smetacek & Naqvi 2008). Maximum biomass values characterized TARA_123 in the coastal waters of the Nuku Hiva island (33.6 mg m^{-2}), where low salinity values testified an impact of waters of terrestrial origin. Intermediate chlorophyll values of 28.5 mg m^{-2} and 27.6 mg m^{-2} characterized TARA_124 and TARA_125 stations, respectively. The former was in a high-salinity small cyclonic eddy generated by high shear at the southern side of the Nuku Hiva Island, while the latter, ~250 km downstream of the islands, still showed the presence of the chlorophyll patch.

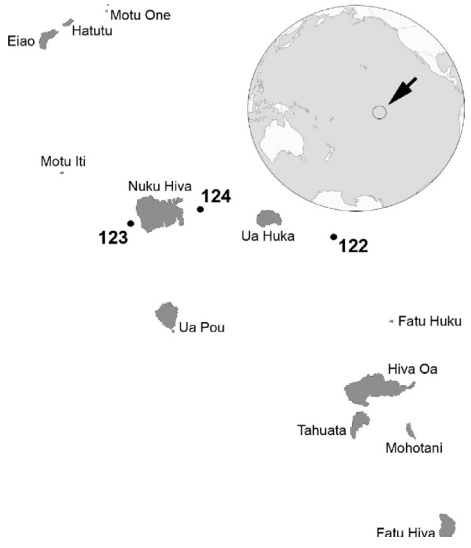

Figure 1. Map of the Marquesas Islands in the Equatorial Pacific with the location of the four stations (TARA_122–125) sampled during the *Tara* Oceans expedition.

Metabarcoding and flow-cytometry data showed that the smallest phytoplankton size fractions were dominated by members of the genera *Synechococcus* and *Prochlorococcus* (Caputi et al. 2019), which matches previous observations (in particular from the BIOSOPE cruise) in a transect across the equatorial central Pacific (Grob et al. 2007). In the same BIOSOPE cruise, 90% of the autotrophic eukaryotes were represented by cells smaller than 5 μm, while near the Marquesas Islands the percentage of larger cells was slightly higher (Masquelier and Vaulot 2008). In the *Tara* Oceans metabarcoding dataset, the smallest eukaryote size fraction (0.8-5 μm) was dominated by dinoflagellates followed by prasinophytes and diatoms (Caputi et al. 2019).

Sampling

Sampling protocols and corresponding detailed information can be found in Karsenti et al. (2011), Pesant et al. (2015), de Vargas et al. (2015) and Sunagawa et al. (2020). Niskin bottle samples were deployed using a rosette. Net-tow samples were collected with a bongo net, concentrated and fractionated into four size classes (0.8–5 μm, 5–20 μm, 20–180 μm, and 180–2,000 μm). Immediately upon collection, phytoplankton samples were preserved either with glutaraldehyde (1% final concentration [f.c.]), buffered formaldehyde solution (2% f.c.), ethanol (95% f.c.) or a mixture of 1% formaldehyde (f.c.) and 0.25% glutaraldehyde (f.c.). The following relevant environmental data were available for the four sites and were used in this study: depth [m], water temperature [°C], salinity [ppt], conductivity [$S \cdot m^{-1}$], abundance [sigma-theta, $kg \cdot m^{-3}$], oxygen [$\mu mol \cdot L^{-1}$] and nitrate [$mg \cdot L^{-1}$] concentrations. Iron concentration estimates [nmol] calculated from the PISCES-v2 model (Aumont et al. 2015) were also available (Caputi et al. 2019).

Aliquots of the preserved samples were obtained from the central repository at the Station Biologique de Roscoff and analyzed during the period from 2011 to 2015. In total, 45 samples from the four *Tara* Oceans stations (TARA_122 to TARA_125) were studied in detail, including samples from two depths, surface (S; 0–5 m) and deep chlorophyll maximum (DCM or D; 150 m), Niskin bottle samples together with three size-fractionated net-tow samples (0.8–5 μm, 5–20 μm, 20–180 μm), and samples preserved in various fixatives (Table 2). Phytoplankton were identified and counted using light microscopy (15 samples), scanning electron microscopy (30 samples), and automated confocal laser scanning microscopy (7 samples).

Light microscopy

Niskin bottle samples and 20-180 μm net samples were analyzed by light microscopy (LM) to estimate phytoplankton total abundance (TA, cells L^{-1}) and relative abundance (RA, %), respectively. For the Niskin bottle samples, preserved in 2% buffered formaldehyde (f.c.), 50 ml were allowed to sediment in an Utermöhl chamber for 3 to 4 days, with calcofluor-white stain (1:100,000). This dye stains cellulose, thus allowing for better detection and identification of thecate dinoflagellates. Cells were identified and enumerated (Utermöhl, 1958) by examining half of the chamber bottom and concentrations per litre ($cells \cdot L^{-1}$) were calculated.

Table 1. Locations and sampling dates of the four stations from the *Tara* Oceans expedition studied here.

Station number	Latitude	Longitude	Sampling Date Start	Sampling Date End
122	-8.9691	-139.3375	26-Jul-2011	29-Jul-2011
123	-8.8785	-140.3036	31-Jul-2011	2-Aug-2011
124	-8.9988	-140.5875	4-Aug-2011	5-Aug-2011
125	-8.8897	-142.6096	8-Aug-2011	9-Aug-2011

Samples from the 20 to 180 μm size-fraction samples from net-tows were fixed with 2% buffered formaldehyde (f.c.) and were examined with the objective of increasing the chances of encountering larger and less common species. Sample volumes of 1–3 ml (depending on cell concentration) (Table 2) were placed in an Utermöhl chamber with calcofluor-white stain (1:100,000) and left to sediment for a couple of hours. Sedimented cells from 2 to 4 transects across the chamber were identified and enumerated. The entire bottom plate was also scanned for rare species. For these samples only relative abundances were obtained (Note: TARA_124_DCM was not available for this analysis).

The LM observations were conducted using inverted light microscopes (Carl Zeiss Axiophot 2 and Leica DMI3000 B) at 400x magnification. Whenever possible, identification was performed at the species level. Taxa that could not be identified to the species or genus level were assigned to suprageneric groups such as centric diatoms, coccolithophores, cryptophyceans, dinoflagellates and other phytoflagellates. For some analyses, autotrophic protists were grouped into 4 groups: diatoms, dinoflagellates, coccolithophores and other phytoplankton.

Scanning electron microscopy

In order to improve species identification, samples from surface and DCM falling into the size classes 0.8–5 μm, 5–20 μm and 20–180 μm were examined by scanning electron microscopy (SEM). Formaldehyde-preserved samples were carefully filtered through 3 μm-pore size Nucleopore™ polycarbonate membrane filters using a Swinnex filter holder (13 mm) screwed on a syringe and gravity sedimentation. Samples were then washed with distilled water, dehydrated in an ethanol series (25%, 50%, 75%, 95% and 100%) and dried using a critical point dryer. Dried filters were mounted on aluminum stubs, sputter-coated with gold-palladium, and observed using Philips 505 and JEOL JSM-6500F electron microscopes.

Formaldehyde-, glutaraldehyde- and ethanol-preserved samples were used for additional detailed examination using JEOL JSM-7401F. Sample preparation varied based on the fixative chemical and due to testing of various protocols. For cryo-sublimation, 1–2 ml of a formaldehyde- or glutaraldehyde-preserved sample was carefully centrifuged in a Millipore™ Ultrafree®-CL Centrifugal Filter Unit with a PVDF membrane (pore size 0.1 μm) for 3 min at 1,000 rpm. After that, the pellet was incubated for 5 min in 1 ml of sterile seawater, and again centrifuged for 2–3 min at 1,000 rpm. Throughout the procedure, it was ensured that the filter did not get completely dry. This washing step was repeated 3 times. Next, the sample was post-fixed for 30 min with a mixture of 2% OsO_4 in 0.5 ml sterile sea water and centrifuged for 2 min at 1,000 rpm. It was then washed 3 times as described above. Finally, the centrifugation unit was cut open and the membrane with the sample was quickly but carefully removed and placed immediately into liquid nitrogen. Cryo-sublimation took place in a cryo-attachment Alto2500 (Gatan) connected directly with SEM or in a modified freeze dryer evacuated with a rotary pump for 5-6 hrs. In the critical point drying protocol, the first steps were identical with the cryo-sublimation procedure up to the post-fixation step with 2% OsO_4. Post-fixed samples were dropped onto coverslips coated with polylysine and were dehydrated in an acetone series (30%, 50%, 70%, 80%, 90%, 95%, and 100%). Ethanol-preserved samples were transferred directly into 100% ethanol and dried using a critical point dryer machine. Regardless of the preparation method, dried filters were mounted on aluminum stubs, sputter-coated with gold-palladium and examined by SEM. For subsequent taxonomical assessment, over 4,000 SEM images from 30 samples were generated, which are now publicly available along with their annotation (Zingone et al., 2022; https://www.ebi.ac.uk/biostudies/bioimages/studies/S-BIAD598).

Environmental high content fluorescence microscopy

Surface net-tow 5–20 μm samples preserved in a formaldehyde-glutaraldehyde mixture, and assigned for high-throughput microscopy, were quantitatively examined by environmental High Content Fluorescence Microscopy (eHCFM), an automated confocal laser scanning microscopy technique described in detail in Colin et al. (2017). Key cellular features were labelled with various dyes: DNA/nuclei (blue, Hoechst 33342); (intra)cellular membranes (green, $DiOC_6$); cell covers and extensions (PLL-AF546, a home-made conjugation between α-poly-L-lysine (PLL) and Alexa Fluor 546 (AF546)); chloroplasts (red, chlorophyll autofluorescence). The image acquisition was conducted on a Leica TCS SP8 confocal laser scanning microscope with a 40x water immersion objective. Five channels were recorded for each encountered object, namely transmitted light and four fluorescent channels (respectively for Hoechst, $DiOC_6$, AF546, and chlorophyll *a*). For detailed information about methodology, see Colin et al. (2017). The resulting sets of images (~1500–5000 images/sample), publicly available at the web-database EcoTaxa (Picheral et al., 2017, Colin 2022; https://ecotaxa.obs-vlfr.fr/prj/3330), were automatically classified based on morphological similarities into morpho-taxonomical categories using supervised machine learning predictions. However, a thorough visual inspection was performed for curating the taxonomical assessment. A final list of phytoplankton taxa identified in the examined samples was compiled from all microscopic techniques (LM, SEM, confocal microscope), including presence/absence data for each taxon.

Identification

Specimens observed in LM and SEM were identified based on classic taxonomy textbooks (Cupp 1943; Rampi and Bernard, 1980; Dodge 1982; Tomas 1997) complemented by numerous more recent papers concerning specific genera and species. To assure quality and comparability of the phytoplankton taxonomic data, we followed the procedures described by Zingone et al. (2015). In particular, the encountered taxa were attributed a species name in all cases when the attribution was based on the appropriate method (i.e., LM or SEM when needed) and all images needed (e.g., full plate pattern in case of dinoflagellates that require it for a reliable attribution). Otherwise, the species or genus names were preceded by 'cf.', meaning that an unambiguous identification was not possible because of inappropriate method or missing morphological information. In case the species was similar to but clearly different from a known taxon, the

Table 2. Schematic explanation of data sets D1–D3 used for statistical analyses. eHCFM = environmental high content fluorescence microscopy, LM = light microscopy, SEM = scanning electron microscopy.

Data set code	Method used	Procedure	Type of sample (size fraction)	Sample acronym	Total numbers observed	Collapsed number of taxa to higher taxon. groups
D1	eHCFM	taxonomic count	net sample (5-20 μm)	N5	209 taxa	81 genera
	LM	taxonomic count	net sample (20-180 μm)	N20		
D2	LM	taxonomic count	bottle sample (unfractionated)	B	209 taxa	81 genera
D3	LM +eHCFM +SEM	presence/ absence data	all of the above (N5 +N20+B) and SEM data	ALL-M	288 taxa	4 gross taxonomic groups

species or genus name was preceded by 'aff.' The use of these 'open taxonomy' qualifiers allows to disclose the uncertainty of the identification without losing potentially useful morphological information (Bengtson 1988). The valid species names were checked using the WORM 'match taxa' tool (https://www.marinespecies.org/aphia.php?p=match) and the results were refined following the most recent taxonomic literature. Finally, the high number of pictures taken during microscopy observations to document identifications will allow for their check and revisions in the future thanks to their availability in the public repository BioImages (accession numbers S-BIAD598 and S-BIAD595) as commented in the next section.

Accessibility of images and annotations dataset

Both SEM and eHCFM image datasets with the taxonomical annotations are publicly available. They can be explored and downloaded at the BioImage repository (EBI), respectively at the URLs; https://www.ebi.ac.uk/biostudies/bioimages/studies/S-BIAD598 (Zingone et al., 2022), and; https://www.ebi.ac.uk/biostudies/bioimages/studies/S-BIAD595 (Colin, 2022). All image files and supplementary files are listed individually in the main data table with the annotations and the associated metadata. Using the search bar of the data panel, the files can be filtered according to filename, the annotation, or several metadata (station, depth, size range, sample barcode, fixative, imaging method), and the selection can be downloaded or visualized online.

The SEM dataset (S-BIAD598) can be explored taxonomically from column 5 (finest annotation) and 6 (main taxonomic group) and can be filtered according to the taxonomic names of these two columns within the search bar. The eHCFM dataset (S-BIAD595) can be explored the same way, and lineages can be used for filtering within the search bar. Additionally, two important tables are located at the end of the list. While the first one shows a quantitative summary of the abundance within different taxomonical and morphological categories, the second table lists all these categories and their parental relationship. Each name is a node of a hierarchical framework. In order to promote interoperability with environmental sequence dataset, the taxonomic annotations follow, as far as possible, the taxonomic framework of the UniEuk/EukRibo project (https://doi.org/10.1111/jeu.12414; 2022, https://doi.org/10.5281/zenodo.6896896) (Berney et al. 2017), and Adl et al. (2019). While the species names are not modified, the nomenclature of some key taxonomic nodes can change, e.g. Bacillariophyceae (diatom DI), Dinophyceae (dinoflagellate DN), and Coccolitophorea (coccolithophore CO) become Diatomeae, Dinoflagellata, and Prymnesiophyceae, respectively.

Comparisons between metabarcoding and morphological data

Metabarcoding data from the TARA V9 fragment of the 18S rRNA sequences (V9) obtained and annotated previously (de Vargas et al. 2015) were used to compare phytoplankton composition between the molecular and morphological data. For a comparison at the group level, relative abundance data for the four main phytoplankton groups recognized in LM were extracted from the V9 datasets of the size fractions 5–20 μm and 20-180 μm and compared with the morphological data obtained with eHCFM and LM, respectively. At a lower taxonomic level, the relative abundance data (RA) of diatom taxa in the LM datasets of the 20-180 μm size fraction was compared with read data from the

Table 3. Total number of species and infraspecific taxa within individual taxonomic groups and their totals (S = surface and D = deep chlorophyll maximum).

Taxonomic group	122		123		124		125	
	S	D	S	D	S	D	S	D
Bacillariophyceae	52	46	56	43	60	9	44	35
Dinophyceae	88	69	68	65	85	2	85	82
Prymnesiophyceae	3	2	5	5	6	2	6	1
Other phytoplankton groups	1	3	2	3	5	2	2	5
Total number of taxa	**144**	**120**	**131**	**116**	**156**	**15**	**137**	**123**

Table 4. List of taxa encountered in samples from four stations (TARA 122–125) at two depths, surface (S) and deep chlorophyll maximum (D), with presence (1) or absence (0) in the samples. 'cf.': ambiguous identification; 'aff.': similar to but clearly different from the taxon; 'spp.' may also include a species present in the list but not recognizable due to the limitation of the method used (i.e., key feature/s not visible).

	Station	**122**		**123**		**124**		**125**	
	Depth	**S**	**D**	**S**	**D**	**S**	**D**	**S**	**D**
Bacillariophyceae									
Actinocyclus intermedius	Usoltseva & Khursevich	1	0	1	1	1	0	1	1
Actinocyclus sagittulus	Villareal	1	1	0	0	0	0	1	1
Actinocyclus spp.	Ehrenberg	0	0	1	1	0	0	0	0
Amphora sp.	C.G. Ehrenberg ex F.T. Kützing	0	1	1	0	1	0	0	0
Arcocellulus cornucervis	G.R.Hasle	1	0	0	0	0	0	0	0
Asterolampra marylandica	Ehrenberg	1	0	1	0	1	0	0	0
Asteromphalus arachne	(Brébisson) Ralfs	0	0	0	1	0	0	0	0
Asteromphalus elegans	Greville	1	1	1	1	1	0	1	0
Asteromphalus flabellatus	(Brébisson) Greville	0	0	1	0	1	0	1	0
Asteromphalus heptactis	(Brébisson) Ralfs	1	1	0	1	1	0	1	1
Asteromphalus hiltonianus	(Greville) Ralfs in Pritchard	1	0	0	0	1	0	0	0
Asteromphalus hookeri	Ehrenberg	0	0	0	0	0	0	0	1
Asteromphalus hyalinus	Karsten	0	0	1	0	0	0	0	0
Asteromphalus imbricatus	G.C.Wallich	0	0	0	1	1	0	0	0
Asteromphalus parvulus	Karsten	0	0	0	0	0	0	1	0
Asteromphalus sarcophagus	Wallich	1	1	0	0	0	0	0	1
Asteromphalus stellatus	(Greville) Ralfs in Pritchard	1	0	1	1	1	0	1	0
Azpeitia cf. *antiqua*	(Pantocsek) P.A. Sims in Fryxell	0	0	0	0	1	0	0	0
Azpeitia barronii	G. Fryxell & T. P. Watkins in Fryxell	1	1	1	0	1	0	1	1
Azpeitia nodulifera	(A.W.F.Schmidt) G.A.Fryxell & P.A.Sims	1	1	1	1	1	1	1	1
Bacteriastrum elongatum	Cleve	1	1	0	0	1	0	0	0
Bacteriastrum furcatum	Shadbolt	0	0	0	1	0	0	0	0
Bacteriastrum hyalinum	Lauder	1	1	0	0	0	0	0	0
Bacteriastrum spp.	G. Shadbolt	1	1	1	1	1	0	0	0
Cerataulina pelagica	(Cleve) Hendey	0	1	1	0	0	0	0	1
Chaetoceros atlanticus	Cleve	1	1	0	0	1	0	1	0
Chaetoceros atlanticus var. *neapolitanus*	(Schroeder) Hustedt	1	0	0	0	1	0	0	0
Chaetoceros bacteriastroides	G.H.H.Karsten	1	1	0	1	1	0	0	0
Chaetoceros danicus	Cleve	0	0	0	0	1	0	0	0
Chaetoceros dichaeta	Ehrenberg	1	0	0	0	1	0	1	0
Chaetoceros didymus	Ehrenberg	0	0	0	0	1	0	0	0
Chaetoceros diversus	Cleve	0	1	0	0	0	0	0	0

(*continued on next page*)

Table 4 (*continued*)

	Station	122		123		124		125	
	Depth	**S**	**D**	**S**	**D**	**S**	**D**	**S**	**D**
Chaetoceros lorenzianus	Grunow	0	0	0	0	1	0	1	0
Chaetoceros peruvianus	Brightwell	0	0	1	0	1	0	1	0
Chaetoceros protuberans	Lauder	0	0	1	0	0	0	0	0
Chaetoceros simplex	Ostenfeld	0	0	0	0	1	0	0	0
Chaetoceros spp.	C.G. Ehrenberg	1	1	1	1	1	1	1	1
Cylindrotheca closterium	(Ehrenberg) Reimann & J.C.Lewin	1	1	1	1	1	0	1	1
Dactyliosolen spp.	A.F. Castracane	0	0	1	1	1	0	0	0
Fragilariopsis doliolus	(Wallich) Medlin & P.A.Sims	1	1	1	1	1	0	1	1
Fragilariopsis spp.	F. Hustedt in A. Schmidt et al.	1	1	1	1	1	1	1	1
Haslea wawrikae	(Hustedt) Simonsen	1	1	0	0	1	0	0	0
Haslea spp.	R. Simonsen	1	1	1	1	1	0	1	1
Hemiaulus sp.	P.A.C. Heiberg	0	0	1	0	0	0	0	0
Hemidiscus cuneiformis	Wallich	1	1	1	1	1	0	1	1
Lauderia annulata	Cleve	0	0	1	0	0	0	0	0
Leptocylindrus minimus	Gran	0	1	1	0	0	0	0	0
Licmophora sp.	C.A. Agardh	0	0	1	0	0	0	0	0
Lioloma delicatulum	(Cupp) Hasle	0	0	1	0	0	0	0	0
Lioloma elongatum	(Grunow) Hasle	1	0	1	0	1	0	1	0
Lioloma pacificum	(Cupp) Hasle	1	0	1	1	1	0	0	0
Lioloma spp.	Hasle	1	1	1	1	1	1	1	1
Navicula spp.	J.B.M. Bory de Saint-Vincent	1	1	1	1	0	1	0	0
Other Naviculales		1	1	1	1	1	1	1	1
Neomoelleria cornuta	(Cleve) S.Blanco & C.E.Wetzel	0	0	1	0	0	0	0	0
Nitzschia bicapitata	Cleve	1	1	1	1	1	0	0	1
Nitzschia ikeanae	Fryxell & Lee in Lee & Fryxell	0	1	0	0	0	0	1	0
Nitzschia longissima	(Brébisson) Ralfs	1	1	1	1	1	0	1	0
Nitzschia longissima var. reversa	Grunow	0	1	1	1	1	0	0	0
Nitzschia spp.	A.H. Hassall	1	1	1	1	1	0	1	1
cf. *Pachyneis*	R. Simonsen	1	0	0	0	0	0	0	0
Phaeodactylum tricornutum	Bohlin	0	0	0	0	0	0	1	0
Plagiotropis lepidoptera	(Gregory) Kuntze	0	1	0	0	0	0	0	0
Plagiotropis sp.	E. Pfitzer	0	0	1	0	0	0	0	0
Planktoniella sol	(C.G.Wallich) Schütt	1	1	1	1	1	0	1	1
Pleurosigma sp.	W. Smith	1	0	1	1	1	0	1	1
Proboscia alata	(Brightwell) Sundström	0	0	0	0	1	0	1	0

(*continued on next page*)

Table 4 (*continued*)

	Station	122		123		124		125	
	Depth	S	D	S	D	S	D	S	D
Pseudo-nitzschia aff. *delicatissima*	(Cleve) Heiden	1	1	1	1	1	0	0	1
Pseudo-nitzschia aff. s*eriata*	(Cleve) H.Peragallo	1	0	1	1	1	1	0	0
Pseudo-nitzschia cf. *fraudulenta*	(Cleve) Hasle	1	1	0	0	1	0	0	0
Pseudo-nitzschia cf. *galaxiae*	N.Lundholm & Ø.Moestrup	0	0	0	0	1	0	1	0
Pseudo-nitzschia pseudodelicatissima	(Hasle) Hasle	1	1	0	1	1	0	1	0
Pseudo-nitzschia spp.	H. Peragallo in H. Peragallo & M. Peragallo	1	1	1	1	1	1	1	1
Rhizosolenia bergonii	H.Peragallo	1	1	0	1	1	0	1	1
Rhizosolenia hebetata	Bailey	0	0	0	0	0	0	1	0
Rhizosolenia spp.	T. Brightwell	1	1	1	1	1	0	1	1
Roperia tesselata	(Roper) Grunow ex Pelletan	1	0	1	0	1	0	1	1
Shionodiscus oestrupii	(Ostenfeld) A.J.Alverson	1	1	1	1	1	0	1	1
Shionodiscus oestrupii var. *venrickae*	(G. Fryxell & Hasle) A.J. Alverson	0	0	1	0	0	0	0	0
Skeletonema tropicum	Cleve	0	0	1	0	0	0	0	0
Thalassionema bacillare	(Heiden) Kolbe	0	0	1	0	0	0	0	0
Thalassionema frauenfeldii	(Grunow) Tempère & Peragallo	0	1	1	0	0	0	0	0
Thalassionema nitzschioides	(Grunow) Mereschkowsky	1	1	1	0	1	0	1	1
Thalassiosira aff. *eccentrica*	(Ehrenberg) Cleve	1	1	1	1	1	0	1	1
Thalassiosira eccentrica	(Ehrenberg) Cleve	1	0	1	1	1	0	1	1
Thalassiosira gravida	Cleve	0	0	0	0	0	0	0	1
Thalassiosira profunda	(Hendey) Hasle	1	1	1	1	1	0	0	0
Thalassiosira rotula	Meunier	0	0	0	0	0	0	0	1
Thalassiosira subtilis	(Ostenfeld) Gran	1	1	1	1	1	0	1	1
Thalassiosira spp.	P.T. Cleve	1	1	1	1	1	1	1	1
cf. *Thalassiosira*	P.T. Cleve	1	1	1	1	1	0	1	1
Thalassiothrix gibberula	Hasle	0	0	0	1	1	0	1	1
Triceratium sp.	C.G. Ehrenberg	0	0	0	1	0	0	0	0
Dinophyceae									
Actiniscus pentasterias	(Ehrenberg) Ehrenberg	0	1	1	0	0	0	0	0
Amphidoma languida	Tillmann	0	0	0	0	0	0	0	1
Amphidoma cf. *nucula*	Stein	1	0	0	0	0	0	0	0
Amphidoma cf. *stenii*	Schiller	1	0	0	0	0	0	0	0
Amphisolenia bidentata	Schröder	0	0	0	0	1	0	1	0
Amphisolenia clavipes	Kofoid	1	0	0	0	0	0	0	0
Amphisolenia rectangulata	Kofoid	0	0	0	0	1	0	0	0
Amphisolenia schroederi	Kofoid	0	0	0	0	0	0	0	1

(*continued on next page*)

Table 4 (*continued*)

	Station	122		123		124		125	
	Depth	**S**	**D**	**S**	**D**	**S**	**D**	**S**	**D**
Archaeosphaerodiniopsis verrucosa	Rampi	1	1	1	1	1	0	1	1
Azadinium caudatum	(Halldal) Nézan & Chomérat	1	0	0	0	0	0	0	0
Azadinium spp.	Elbrächter & Tillmann	1	1	1	0	1	0	0	0
Blepharocysta okamurae	Abé	1	0	0	1	0	0	1	1
Blepharocysta splendor-maris	(Ehrenberg) Ehrenberg	0	1	1	1	1	0	0	0
Centrodinium biconicum	(Murray & Whitting) F.J.R.Taylor	0	0	0	0	1	0	0	1
Centrodinium cf. *intermedium*	Pavillard	0	1	0	0	0	0	0	0
Ceratocorys armata	(Schütt) Kofoid	1	1	0	0	0	0	0	0
Ceratocorys horrida	Stein	0	0	0	0	0	0	1	0
Citharistes regius	Stein	0	1	1	1	1	0	0	1
Cladopyxis brachiolata	Stein	1	0	0	0	0	0	0	0
Corythodinium constrictum	(F.Stein) F.J.R.Taylor	1	1	1	1	1	0	1	0
Corythodinium elegans	(Pavillard) F.J.R.Taylor	1	0	0	0	0	0	1	1
Corythodinium milneri	(G.Murray & Whitting) F.Gómez	0	1	0	0	0	0	0	0
Corythodinium strophalatum	(J.D.Dodge & R.D.Saunders) F.Gómez	0	0	0	0	0	0	0	1
Corythodinium tesselatum	(F.Stein) Loeblich Jr. & Loeblich III	1	1	1	1	1	0	1	1
Dinophysis amphora	Balech	0	1	0	0	0	0	1	1
Dinophysis cf. *ovum*	(F.Schütt) T.H.Abé	0	0	1	1	0	0	1	1
Dinophysis fortii	Pavillard	1	0	0	0	0	0	0	0
Dinophysis hastata	F.Stein	0	0	0	0	0	0	0	1
Dinophysis pusilla	Jørgensen	0	0	0	0	1	0	0	1
Dinophysis similis	Kofoid & Skogsberg	1	0	0	0	0	0	0	0
Dinophysis schuettii	Murray & Whitting	1	0	0	0	0	0	1	0
Diplopsalis spp.	Bergh	0	0	0	1	0	0	1	0
Dissodinium pseudolunula	Swift ex Elbrächter & Drebes	0	0	0	0	0	0	1	0
Goniodoma polyedricum	(Pouchet) Dodge	1	1	1	1	1	0	1	1
Goniodoma sphaericum	Murray & Whitting	1	0	0	0	0	0	1	0
Gonyaulax birostris	Stein	1	0	0	0	1	0	1	1
Gonyaulax ceratocoroides	Kofoid	0	0	0	0	1	0	0	0
Gonyaulax cf. *fragilis*	(Schütt) Kofoid	1	1	0	1	1	0	1	1
Gonyaulax turbynei	Murray & Whitting	1	0	1	0	0	0	1	0
Gonyaulax fusiformis	H.W.Graham	1	1	0	0	0	0	0	0
Gonyaulax monacantha	Pavillard	0	1	0	0	0	0	0	1
Gonyaulax monospina	Rampi	0	0	0	0	1	0	0	0
Gonyaulax polygramma	F.Stein	1	0	1	0	1	0	1	1
Gonyaulax cf. reticulata	Kofoid & Michener	0	0	0	0	1	0	1	0

(*continued on next page*)

Table 4 (*continued*)

	Station	122		123		124		125	
	Depth	**S**	**D**	**S**	**D**	**S**	**D**	**S**	**D**
Gonyaulax spinifera	(Claparède & Lachmann) Diesing	1	0	1	1	1	0	1	1
Gymnodinium spp.	F. Stein	1	1	0	0	1	0	1	1
Gyrodinium spp.	Kofoid & Swezy	0	0	1	0	0	0	0	0
Heterodinium milneri	(Murray & Whitting) Kofoid	0	1	0	0	1	0	0	1
Histioneis aff. *gubernans*	Schütt	1	0	0	0	1	0	0	0
Histioneis cymbalaria	Stein	0	0	0	0	1	0	0	1
Histioneis depressa	Schiller	1	0	0	0	0	0	0	0
Histioneis elongata	Kofoid & Michener	0	1	0	0	1	0	0	1
Histioneis hyalina	Kofoid & Michener	0	0	0	1	0	0	0	1
Histioneis longicollis	Kofoid	0	0	0	1	1	0	0	0
Histioneis milneri	Murray & Whitting	0	0	0	0	1	0	0	0
Histioneis oxypteris	Schiller	0	0	0	0	0	0	1	0
Histioneis panaria	Kofoid & Skogsberg	1	0	0	0	0	0	0	0
Histioneis panda	Kofoid & Michener	0	0	0	0	0	0	1	0
Histioneis pietschmannii	Böhm	0	0	0	0	1	0	0	1
Histioneis rotundata	Kofoid & Michener	1	1	1	1	1	0	0	0
Histioneis variabilis	Schiller	0	1	0	1	0	0	1	1
Karenia spp.	G.Hansen & Moestrup	0	1	0	0	0	0	0	0
Karlodinium spp.	J.Larsen	1	1	1	1	1	0	1	1
Lingulodinium polyedra	(F.Stein) J.D.Dodge	1	0	0	0	0	0	1	0
Lissodinium spp.	Matzenauer	0	0	1	1	1	0	1	0
Mesoporos perforatus	(Gran) Lillick	1	1	1	1	1	0	1	1
Ornithocercus carolinae	Kofoid	0	0	0	0	1	0	0	0
Ornithocercus magnificus	Stein	1	1	1	1	1	0	1	0
Ornithocercus quadratus	Schütt	1	0	0	1	1	0	0	1
Ornithocercus steinii	Schütt	0	0	0	0	1	0	1	1
Ornithocercus thurnii	(Schmidt) Kofoid & Skogsberg	0	0	1	0	1	0	0	0
Oxytoxum caudatum	Schiller	1	1	0	0	1	0	0	0
Oxytoxum crassum	J.Schiller	1	1	1	1	1	0	1	1
Oxytoxum curvatum	(Kofoid) Kofoid & J.R.Michener	1	1	1	1	0	0	1	1
Oxytoxum globosum	Schiller	0	1	1	0	1	0	0	0
Oxytoxum laticeps	Schiller	1	1	1	1	1	0	1	1
Oxytoxum sceptrum	(F.Stein) Schröder	1	1	0	0	0	0	1	1
Oxytoxum scolopax	Stein	1	1	1	1	1	0	1	1
Oxytoxum turbo	Kofoid	0	0	1	0	0	0	1	0
Oxytoxum variabile	Schiller	1	1	1	1	1	0	1	1

(*continued on next page*)

Table 4 (*continued*)

	Station	122		123		124		125	
	Depth	**S**	**D**	**S**	**D**	**S**	**D**	**S**	**D**
Oxytoxum spp.	Stein	0	1	1	1	0	0	1	1
Palaeophalacroma unicinctum	J.Schiller	1	1	1	1	1	0	1	1
Palaeophalacroma verrucosum	Schiller	0	0	0	0	0	0	0	1
Pentapharsodinium tyrrhenicum	(Balech) Montresor	0	0	0	0	0	0	1	0
Phalacroma doryphorum	Stein	1	1	0	1	1	0	0	0
Phalacroma parvulum	(Schütt) Jörgensen	0	0	0	0	1	0	0	0
Phalacroma rotundatum	(Claparéde & Lachmann) Kofoid & J.R.Michener	0	1	1	1	1	0	1	1
Podolampas bipes	Stein	1	1	1	0	1	0	1	1
Podolampas elegans	Schütt	1	1	1	1	0	0	0	0
Podolampas palmipes	Stein	1	1	1	1	1	0	1	1
Podolampas spinifera	Okamura	1	1	1	1	0	0	1	1
Pronoctiluca spp.	Fabre-Domergue	1	1	0	1	1	0	1	1
Prorocentrum balticum	(Lohmann) Loeblich III	1	1	1	1	1	0	1	1
Prorocentrum compressum	(Bailey) T.H.Abé ex J.D.Dodge	1	1	1	1	1	0	1	1
Prorocentrum dentatum	Stein	1	1	1	1	1	0	1	1
Prorocentrum cf. *hoffmannianum*	M.A.Faust	1	0	0	0	0	0	1	0
Prorocentrum micans	Ehrenberg	1	0	1	1	0	0	0	1
Prorocentrum minimum	(Ostenfeld) J.D.Dodge	1	1	0	1	0	0	1	1
Prorocentrum cf. *nux*	Puigserver & Zingone	1	0	1	0	1	1	1	0
Prorocentrum triestinum	J.Schiller	1	0	1	0	0	0	0	0
Protoceratium areolatum	Kofoid	0	0	0	0	0	0	0	1
Protoceratium reticulatum	(Claparède & Lachmann) Bütschli	0	0	0	1	0	0	0	1
Protoceratium spinulosum	(Murray & Whitting) Schiller	1	0	0	0	1	0	1	0
Protoperidinium abei	(Paulsen) Balech	0	0	0	1	0	0	0	0
Protoperidinium brevipes	(Paulsen) Balech	0	0	1	1	0	0	0	1
Protoperidinium conicum	(Gran) Balech	1	1	1	1	1	0	1	0
Protoperidinium crassipes	(Kofoid) Balech	0	0	0	0	0	0	1	0
Protoperidinium depressum	(Bailey) Balech	1	0	0	0	0	0	1	0
Protoperidinium diabolus	(Cleve) Balech	0	1	1	0	0	0	1	0
Protoperidinium globulus	(Stein) Balech	1	0	0	0	1	0	0	1
Protoperidinium cf. *granii*	(Ostenfeld) Balech	1	0	0	0	0	0	0	0
Protoperidinium latissimum	(Kofoid) Balech	1	1	0	0	0	0	0	0
Protoperidinium cf. *leonis*	(Pavillard) Balech	0	0	0	1	1	0	0	1
Protoperidinium oceanicum	(VanHöffen) Balech	0	0	0	0	0	0	0	1
Protoperidinium oviforme	(Dangeard) Balech	1	1	1	0	0	0	1	1

(*continued on next page*)

Table 4 (*cortinued*)

	Station	122		123		124		125	
	Depth	**S**	**D**	**S**	**D**	**S**	**D**	**S**	**D**
Protoperidinium ovum	(Schiller) Balech	0	0	1	1	0	0	0	0
Protoperidinium pallidum	(Ostenfeld) Balech	0	1	0	0	0	0	0	0
Protoperidinium pentagonum	(Gran) Balech	0	1	0	0	0	0	1	0
Protoperidinium pyriforme	(Paulsen) Balech	1	0	0	1	1	0	1	1
Protoperidinium pyriforme var. breve	(Paulsen) Balech	0	0	0	1	0	0	0	0
Protoperidinium quarnerense	(B.Schröder) Balech	1	0	1	1	1	0	1	1
Protoperidinium cf. *sinaicum*	(Matzenauer) Balech	0	1	0	0	0	0	0	0
Protoperidinium cf. *sphaericum*	(Murray & Whitting) Balech	0	0	1	0	0	0	0	0
Protoperidinium cf. *steinii*	(Jørgensen) Balech	0	0	1	1	1	0	1	1
Protoperidinium cf. *thulesense*	(Balech) Balech	1	0	0	0	0	0	0	0
Protoperidinium cf. *tuba*	(Schiller) Balech	0	1	0	0	0	0	0	0
Protoperidinium spp.	Bergh	1	1	1	1	1	0	1	1
Ptychodiscus noctiluca	Stein	0	0	0	0	0	0	1	0
Pyrocystis elegans	Pavillard	1	1	0	1	1	0	0	1
Pyrocystis fusiformis	C.W.Thomson	0	0	0	0	1	0	0	1
Pyrocystis gerbaulti	Pavillard	0	1	0	0	1	1	1	1
Pyrocystis hamulus	Cleve	0	1	0	0	0	0	0	0
Pyrocystis lunula	(Schütt) Schütt	1	1	1	0	0	0	1	1
Pyrocystis obtusa	Pavillard	1	1	0	0	1	0	1	1
Pyrocystis robusta	Kofoid	1	0	0	0	0	0	1	1
Pyrophacus steinii	(Schiller) Wall & Dale	1	0	1	1	0	0	0	0
Scrippsiella acuminata	(Ehrenberg) Kretschmann	1	0	0	1	0	0	1	1
Scrippsiella spp. s*ensu lato*	Balech ex A.R.Loeblich III	1	1	1	1	1	0	1	1
Spiraulax jolliffei	(Murray & Whitting) Kofoid	0	0	0	0	1	0	0	1
Tripos arietinus	(Cleve) F.Gómez	1	0	0	0	0	0	1	0
Tripos azoricus	(Cleve) F.Gómez	0	0	1	0	0	0	0	0
Tripos brevis	(Ostenfeld & Johannes Schmidt) F.Gómez	1	0	1	1	1	0	1	1
Tripos candelabrus	(Ehrenberg) F.Gómez	1	0	1	1	0	0	1	1
Tripos carnegiei	(H.W.Graham et Bronikovsky) F.Gómez	0	0	0	0	1	0	0	0
Tripos carriensis	(Gourret) F.Gómez	0	0	0	0	0	0	0	1
Tripos cephalotus	(Lemmermann) F.Gómez	0	0	0	0	0	0	0	1
Tripos concilians	(Jørgensen) F.Gómez	0	0	1	0	0	0	1	0
Tripos contortus	(Gourret) F.Gómez	0	1	0	0	0	0	0	0
Tripos declinatus	(G.Karsten) F.Gómez	1	1	0	1	1	0	1	1
Tripos digitatus	(F.Schütt) F.Gómez	0	0	1	0	0	0	0	0

(*cortinued on next page*)

Table 4 (*continued*)

	Station	122		123		124		125	
	Depth	**S**	**D**	**S**	**D**	**S**	**D**	**S**	**D**
Tripos euarcuatus	(Jørgensen) F.Gómez	0	0	1	0	0	0	0	0
Tripos furca	(Ehrenberg) F.Gómez	1	1	1	1	1	0	1	1
Tripos fusus	(Ehrenberg) F.Gómez	1	1	1	1	1	0	1	1
Tripos gibberus	(Gourret) F.Gómez	1	0	1	0	0	0	1	0
Tripos gravidus	(Gourret) F.Gómez	0	0	0	0	1	0	0	0
Tripos kofoidii	(E.G.Jørgensen) F.Gómez	0	0	1	0	1	0	0	0
Tripos limulus	(Pouchet) F.Gómez	1	0	1	1	1	0	1	0
Tripos cf. *lineatus*	(Ehrenberg) F.Gómez	0	0	0	1	1	0	1	0
Tripos longipes	(Bailey) F.Gómez.	0	1	0	0	0	0	0	0
Tripos longirostrum	(Gourret) Hallegraeff & Huisman	0	1	0	1	1	0	0	0
Tripos macroceros	(Ehrenberg) F.Gómez	1	0	0	0	1	0	0	1
Tripos massiliense	(Gourret) F.Gómez	0	0	0	1	1	0	1	0
Tripos minutus	(E.G.Jørgensen) F.Gómez	1	0	1	0	0	0	1	1
Tripos muelleri	Bory de Saint-Vincent	1	0	0	1	1	0	0	0
Tripos muelleri var. atlantica	(Ostenfeld) F.Gómez	0	0	0	0	1	0	1	0
Tripos muelleri f. parallela	(Schmidt) F.Gómez	0	0	1	0	0	0	0	0
Tripos cf. *pacificus*	(Schröder) F.Gómez	0	0	0	0	1	0	0	0
Tripos paradoxides	(Cleve) F.Gómez	0	0	0	0	1	0	0	0
Tripos pentagonus	(Gourret) F.Gómez	1	1	1	1	1	0	1	1
Tripos protuberans	(G.Karsten) F.Gómez	1	0	0	0	0	0	0	1
Tripos setaceus	(Jørgensen) F.Gómez	1	1	1	0	0	0	0	0
Tripos symmetricus	(Pavillard) F.Gómez	0	0	1	0	0	0	0	0
Tripos teres	(Kofoid) F.Gómez	1	1	1	1	1	0	1	1
Tripos trichoceros	(Ehrenberg) Gómez	0	0	0	0	1	0	1	1
Prymnesiophyceae									
Calcidiscus leptoporus	(G.Murray & V.H.Blackman) Loeblich Jr. & Tappan	1	0	0	1	1	1	1	0
Calciosolenia spp.	Gran	0	0	1	0	1	0	1	1
Emiliania huxleyi	(Lohmann) W.W.Hay & H.P.Mohler	0	1	0	0	1	1	1	0
Gephyrocapsa oceanica	Kamptner	1	0	1	0	1	0	1	0
Michaelsarsia elegans	Gran	0	0	1	0	0	0	0	0
Oolithotus antillarum	(Cohen) Cohen & P.Reinhardt	0	0	0	1	0	0	1	0
Pontosphaera syracusana	Lohmann	0	0	0	0	1	0	0	0
Syracosphaera pulchra	Lohmann	0	0	0	1	0	0	0	0
Umbellosphaera spp.	Paasche	1	1	1	1	0	0	0	0
Umbilicosphaera sibogae	(Weber Bosse) Gaarder	0	0	0	0	1	0	1	0

(*continued on next page*)

Table 4 (*cortinued*)

	Station	122		123		124		125	
	Depth	S	D	S	D	S	D	S	D
Prymnesium neolepis	(M.Yoshida et al.) Edvardsen, Eikrem & Probert	0	0	0	1	0	0	0	0
Phaeocystis scrobiculata	Ø.Moestrup	0	0	1	0	0	0	0	0
Other phytoplankton									
Dictyocha fibula	Ehrenberg	0	0	1	1	1	1	0	0
Dictyocha spp.	Ehrenberg	1	1	0	1	1	1	0	1
Leucocryptos cf. *marina*	(Braarud) Butcher	0	0	1	0	0	0	0	0
Octactis octonaria	(Ehrenberg) Hovasse	0	1	0	0	0	0	0	1
Pterosperma cf. *rotondum*	Pouchet	0	0	0	0	1	0	0	0
Pterosperma cristatum	Schiller	0	0	0	0	0	0	1	0
Pterosperma marginatum	Gaarder	0	0	0	0	0	0	0	1
Pterosperma michaelsarsii	(Gaarder) Parke & Boalch	0	0	0	1	1	0	0	0
Pterosperma spp.	Pouchet	0	1	0	0	1	0	0	1
Trichodesmium sp.	Ehrenberg ex Gomont	0	0	0	0	0	0	1	1

corresponding diatom V9 dataset obtained previously (Malviya et al. 2016).

Data analysis

Altogether, four independent datasets were obtained from various microscopic approaches: LM counts from the bottle samples (further referred to as B), LM counts from net-tow samples (20–180 μm size class, further referred to as N20), eHCFM counts from net-tow samples (size class of 5–20 μm, further referred to as N5) and acquired presence/absence data from a combination of all SEM and other microscopic examinations (LM + eHCFM + SEM, further referred to as ALL-M; Table 2; Suppl. Table 1). Almost no taxa were noted during examinations of the smallest size fraction (0.8–5 μm). After checking that the absolute counts were proportional in both filtered datasets, data acquired from counting the two larger size fractions (N5 and N20) were summed (Table 2; Suppl. Table 1) to adequately represent a total count for each sample. In addition, the summed counts were each adjusted from the original, most detailed taxonomic assessment (datasets B and N5+N20, each with 209 taxa, ALL-M with 288 taxa) to a dataset with taxa aggregated at the generic level (N5+N20 = dataset D1, and B = dataset D2, each containing 81 taxa) or collapsed into four gross taxonomic groups (ALL-M = dataset D3). This aggregation was performed to reduce noise in the data and the high number of response variables.

The resulting datasets were used to examine variation in phytoplankton communities between sampling depths and among sampling stations, as well as to assess the effects of environmental parameters. Moreover, an assurance test of whether the summed dataset of N5+N20 sample counts provided coherent information in comparison with the B samples was performed. Counts of individual cells and/or taxonomic richness were ln-transformed and standardized to a unit norm in all samples before the analyses. Principal components analysis (PCA) was performed in R, using the R package *vegan* (Oksanen et al., 2007). The full code as well as the data used to perform the analysis can be found in Supplementary Material 1.

Results

Diversity

In total, 289 planktonic protist taxa were identified in pelagic samples collected in the vicinity of the

Table 5. Acronyms and complete names (in grey) used in the ordination diagrams. DI = diatom (Bacillariophyceae), DN = dinoflagellate (Dinophyceae), CO = coccolithophore (Prymnesiophyceae), OT = other phyla.

Acronym	Phylum	Taxon name	Acronym	Phylum	Taxon name
Actinocy	DI	*Actinocyclus*	Navicula	DI	*Navicula*
Azadiniu	DN	*Azadinium*	Nitzschi	DI	*Nitzschia*
Bacteria	DI	*Bacteriastrum*	Oxytoxum	DN	*Oxytoxum*
Calciosl	CO	*Calciosolenia*	Palaeoph	DN	*Palaeophalacroma*
CentDiat	DI	centric DI	PennDiat	DI	pennate DI
Chaetocr	DI	*Chaetoceros*	Prorocen	DN	*Prorocentrum*
Dactylio	DI	*Dactyliosolen*	Pseudont	DI	*Pseudo-nitzschia*
Dictyoch	OT	*Dictyocha*	Pterospr	OT	*Pterosperma*
DinfNakd	DN	naked DN	Rhizosol	DI	*Rhizosolenia*
DinfThec	DN	thecate DN	Shionod	DI	*Shionodiscus*
Dinophys	DN	*Dinophysis*	Thal-nema	DI	*Thalassionema*
Gymnodin	DN	*Gymnodinium*	Thal-sira	DI	*Thalassiosira*
Haslea	DI	*Haslea*	Umbellos	CO	*Umbellosphaera*
Lioloma	DI	*Lioloma*	UndCoc	CO	undetermined CO

Marquesas Islands. The most species-rich groups were dinoflagellates (phylum Myzozoa, class Dinophyceae), with 174 species belonging to 41 genera, and diatoms (phylum Ochrophyta, class Bacillariophyceae), represented by 93 taxa falling into 37 genera (Table 3). The most diverse genera within the dinoflagellates were *Tripos* (35 species), *Protoperidinium* (24), *Histioneis* (13) and *Oxytoxum* (10), while for the diatoms these were *Chaetoceros* (12), *Asteromphalus* (11) and *Thalassiosira* (7) (Table 4). Only 10 species of coccolithophores (phylum Haptophyta, class Prymnesiophyceae) and two other prymnesiophytes were identified, each belonging to different genera. The 'other phytoplankton' group (dictyochophytes, prasinophytes, cyanophytes and xanthophytes) contained lower numbers of identified species, contributing a total of 10 taxa to the final count. Acronyms and complete names used in ordinary diagrams are listed in Table 5.

The number of taxa present in each sample varied from 116 to 156 species, apart from one case (TARA_124-D) with much lower numbers (Table 3). While there were small differences between the surface and DCM layers, somewhat higher numbers of species were observed in the surface layer (Table 3). The highest species richness was observed in the surface samples from the bloom station TARA_124 (156 taxa) and the pre-bloom station TARA_122 (144 taxa). The lowest number of species occurred in the deeper layer at TARA_124 with only 15 taxa observed, which was a result of the low number of identified taxa in the bottle sample and the lack of net samples.

When the different approaches to sample observations were compared, bottle samples examined by LM yielded 63 taxa, which is only 22% of the 288 taxa observed in this study. Examination of N20 by LM provided 140 taxa (49% of the total), whereas 126 taxa (44% of the total) were found during the eHCFM analysis of N5. Finally, SEM was most comprehensive, documenting the presence of 181 taxa (63% of the total), of which approximately 50 were not recognized by other methods. This comparison shows that a combination of multiple microscopy methods is able to document much higher species richness than each method alone. We encountered a significant number of unknown yet abundant diatoms and dinoflagellates. Prominently, an unknown robust centric diatom similar to, but probably not belonging to the genus *Thalassiosira*, was frequently observed in most samples (Figs 2a, b; 3a). Moreover, several species apparently belonging to the genus *Thalassiosira* were noted by SEM, but we were unable to identify them using the available literature (Fig. 2c–f). A very interesting member of the genus *Fragilariopsis*, forming linear colonies and having rectangular girdle views, was also commonly observed (Figs 2g, h; 3). Similarly, many dinoflagellates could not be identified. Among them were two small *Oxytoxum* species very similar in shape to *Oxytoxum crassum*, although both with a different and distinct surface pattern (Figs 2i, j; 3c), and a round *Prorocentrum* species with a smooth surface and few large pores (Fig. 2k). Finally, we encountered the dinoflagellate *Archaeosphaerodiniopsis verrucosa* (Figs 2-l; 3d) described in 1943 (Rampi 1943) and unreported

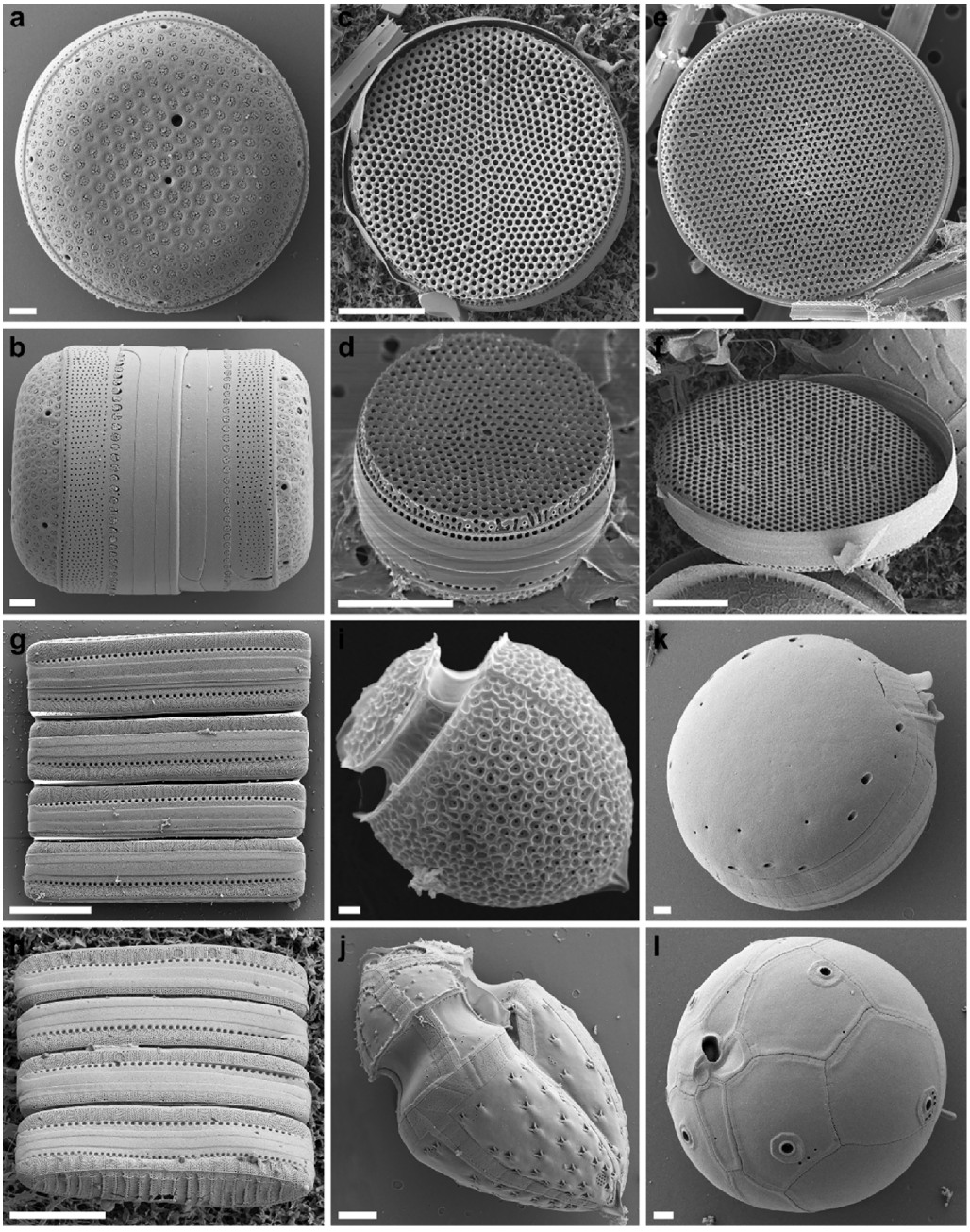

Figure 2. Examples (SEM images) of unidentified diatom (a–h) and dinoflagellate (i–k) taxa encountered in phytoplankton from around Marquesas Islands, and an extremely rare taxon (l). **a**, **b**: cf. *Thalassiosira* (a: valve view, b: girdle view), **c**, **d**: *Thalassiosira* sp.1, **e**, **f**: *Thalassiosira* sp. 2, **g**, **h**: *Fragilariopsis* sp. (colony of 4 cells in girdle view), **i**: *Oxytoxum* sp.1, **j**: *Oxytoxum* sp.2, **k**: *Prorocentrum* sp., **l**: *Archaeosphaerodiniopsis verrucosa*. Scale bars 1 μm (a, b, i–l) and 10 μm (c–h).

ever since. Only very recently Carbonell-Moore (2017) re-discovered this extremely rare taxon in the Central Equatorial Pacific, which corroborates our findings. Surprisingly, this species was encountered in all samples examined by us (Table 4).

Distribution

Phytoplankton abundances were in all cases considerably low, ranging between only 200 cells·L^{-1} and ~18,000 cells·L^{-1} (Fig. 4). The highest cell

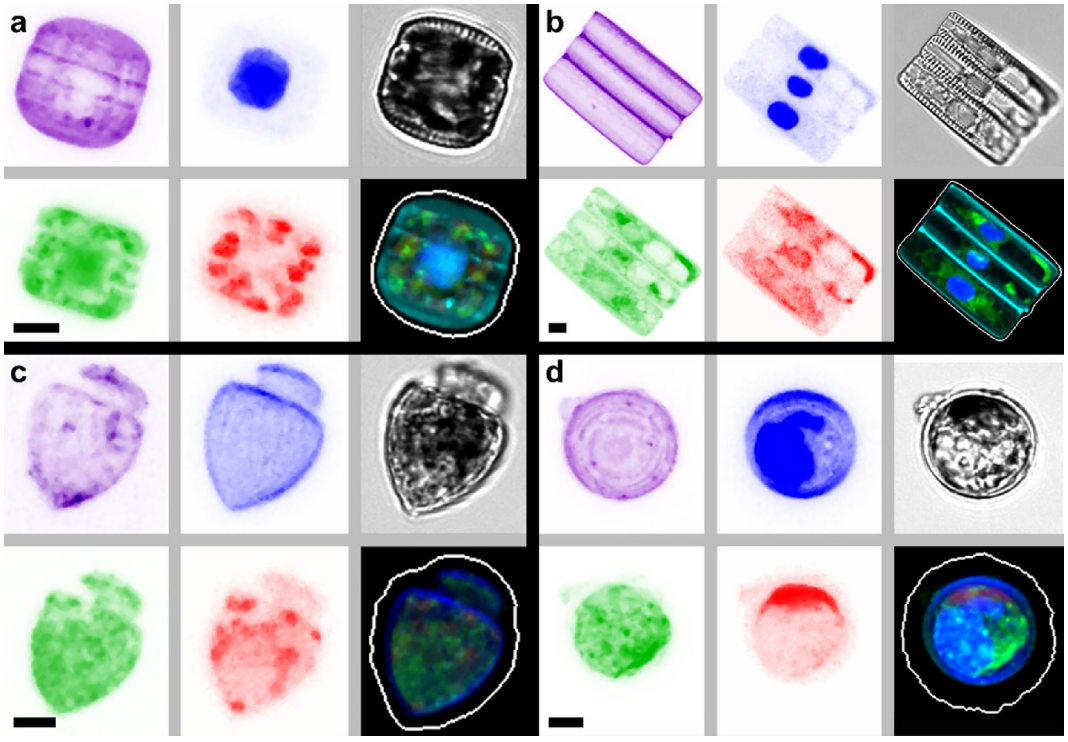

Figure 3. Examples of images of several diatoms (a, b) and dinoflagellates (c, d) taken by confocal microscopy (eHCFM). Each object was depicted in 6 different views (from the top left to the bottom right): purple – surface, blue – DNA/nuclei (it also stained surface in dinoflagellates), black-and-white – light view, green – membranes, red – chlorophyll autofluorescence, all colors – integrated image from all signals. **a**: cf. *Thalassiosira* (girdle view), **b**: *Fragilariopsis* sp. (colony of 3 cells in girdle view; see also Fig. 10 g, h), **c**: *Oxytoxum* sp.1 (see also Fig. 10 i), **d**: *Archaeosphaerodiniopsis verrucosa* (see also Fig. 10 k, l). Scale bars 5 μm.

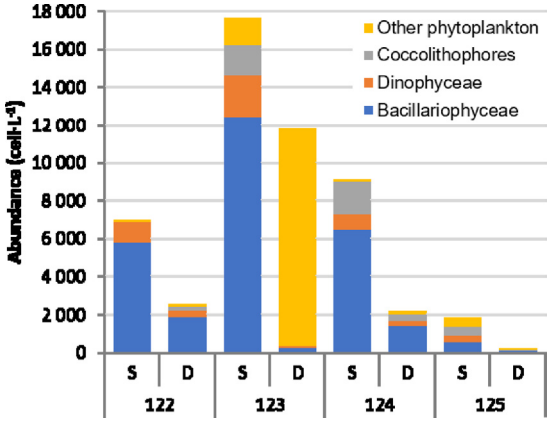

Figure 4. Abundance of the main phytoplankton groups in Niskin bottle samples (LM counts) from four *Tara* Oceans stations (122–125). S = surface, D = deep chlorophyll maximum. Relative abundances from the same data are represented in Fig. 6 (columns marked "B").

abundance was observed in the surface of TARA_123 and TARA_124, both localities with the highest biomass values. When compared to the other locations, the TARA_122 surface sample had intermediate total abundance values of 7,000 cells·L^{-1}, whereas the minima were recorded at TARA_125, far away from the area where blooms generally occur, and where relatively high chlorophyll *a* values were due to higher abundance of picoplankton (Caputi et al. 2019). The deep samples had generally lower abundance (below ~2,000 cells·L^{-1}), but TARA_123 was characterized by relatively high densities (below 12,000 cells·L^{-1}), due to the dominance of small coccoid cells and flagellates (up to 10 μm in size), which we were unable to assign to any phytoplankton group. Bacillariophyceae were relatively abundant in all bottle samples and dominated at TARA_123 and TARA_124 stations (Fig. 4). Species composition was similar among all the samples, yet the relative abundance in individual samples varied among stations and

with depth. Undetermined centric and pennate diatoms, *Cylindrotheca closterium*, as well as *Chaetoceros* and *Pseudo-nitzschia* species were the most abundant diatoms. *Pseudo-nitzschia* species had higher abundance in all surface samples from TARA_122-124, but were not found in the surface sample of TARA_125. *Chaetoceros* species had higher abundance only at TARA_122 and 124 (both depths), while their abundance was close to zero in the other stations. Undetermined centric diatoms and *C. closterium* showed the highest abundance in surface samples fromTARA_123, while undetermined pennate diatoms showed similar abundances in all samples (Fig. 5). *Gephyrocapsa oceanica* was the most abundant coccolithophore at the subsurface of TARA_123.

Relative abundances of taxa from the net-tow sample counts (size fractions 5–20 μm and 20–180 μm) (Fig. 5) were generally similar to each other and to those obtained from Niskin bottle samples (Fig. 6), despite the fact that they were counted from differently collected (bottle vs. net) and processed samples (LM vs. eHCFM). Most of the counted net-tow samples were clearly dominated by diatoms, usually with a contribution of over 50% to each count.

The smaller size fraction (5–20 μm) of both samples from TARA_125, the post-bloom station, was an exception (Fig. 5). Dinoflagellates represented ~10–25% of the plankton in all net-tow samples, excluding the already mentioned small size fractions of TARA_125, in which dinoflagellates dominated, with over 40% of the counted cells. These two samples also contained the highest proportion (~ 30%) of small phytoplanktonic coccoids and flagellates from the group "Other phyla". Furthermore, the deep bottle sample count of TARA_125 seems to completely miss any representatives of the otherwise common group of dinoflagellates, although only 10 encountered cells could be considered (Fig. 6). Finally, coccolithophores occurred in much smaller abundances (Fig. 5) in the net-tow samples compared to the bottle sample counts (Fig. 6).

SEM analysis of the size fraction 0.8–5 μm did not yield any results, as no protists were encountered, except for just three cells of a tiny unknown *Amphora* species (Bacillariophyceae) observed in the TARA_124 surface sample. This taxon was not encountered anywhere else. Since the smallest size fraction did not contain any significant numbers of phytoplankton cells for counts, the size fractions 5–20 μm and 20–180 μm were together considered to account for an adequate representation of the whole sample, and the summed counts were compared to the bottle sample counts (Fig. 6). Several samples showed a very good match in community composition evaluated by different methods (e.g., eHCFM and SEM in both depths of TARA_122).

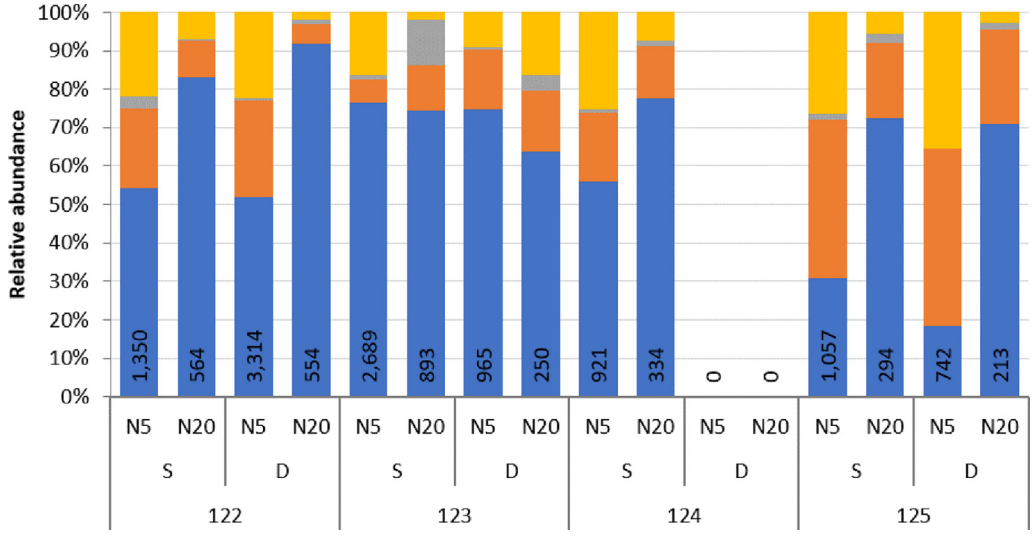

Figure 5. Relative abundances of the main phytoplankton groups in net-tow samples, size fractions of 5–20 μm (N5, using eHCFM) and 20–180 μm (N20, using LM). S = surface, D = deep chlorophyll maximum. Color coding of the groups is the same as in Fig. 4. Values at the base of each bar represent the number of phytoplankton cells counted in each sample. Sample TARA_124 D was not available in either size fraction for enumeration.

On the other hand, several samples did not even contain the same higher taxonomic groups, such as the already mentioned deep TARA_123 sample. A similar situation was found in the deep TARA_125 sample, although this result was apparently skewed by only 10 encountered objects in the un-concentrated bottle sample. Altogether, community composition across the net-tow and bottle samples was similar; diatoms clearly dominated, since in most cases this group represented over 50% of the counted cells. The post-bloom TARA_125 station showed a slightly different pattern with diatoms, dinoflagellates and other phytoplankton being more equally represented (Fig. 6).

Comparison of morphological and molecular data

Comparison of the V9-based estimates of community composition with the eHCFM- and LM-based estimates at the surface and DCM revealed that the V9 data constantly magnified the contribution of Dinophyceae and lessened that of Bacillariophyceae, regardless of the fraction, the station or the depth (Fig. 7). Moreover, the relative weight of the two other categories herein taken into account (namely Prymnesiophyceae and "other phytoplankton groups") was higher when eHCFM was used for the 5-20 μm fraction. In the 20-180 μm fraction, the relative weight of the "other phytoplankton groups" as estimated from the V9 and LM datasets were consistent. Trends in the percentage composition of Bacillariophyceae estimated from the V9- and microscopy-based methods strongly correlate at both the surface and DCM (Figs 5 and 7). However, no correlation was observed for Dinophyceae (surface) and Prymnesiophyceae (DCM) when LM was compared with the V9 data, while V9 vs. LM trends in the same fraction were strongly negatively correlated (Figs 5 and 7).

Considering that the diatoms were the only group for which the taxonomic information was sufficient from both morphological and molecular data, the 20-180 μm size fractions were selected for comparison at a lower taxonomic level, (see Discussion). Since a direct comparison of the RAs showed many discrepancies between the two LM and V9 datasets (data not shown), a sample-by-sample adjustment of the data was required, whereby the RAs of selected taxa were extracted from the V9 dataset based on their presence in the LM dataset. Furthermore, reads lumped into the generic groups in the V9 dataset were reassigned to specific genera. For example, the V9 RA of 'Radial centric basal Coscinodiscophyceae' was matched with LM RAs of *Asterolampra*, *Asteromphalus* and *Hemidiscus* that were not found in the V9 dataset, for the samples where the latter genera were abundant in the LM. Similarly, the V9 sequences labeled as 'raphid

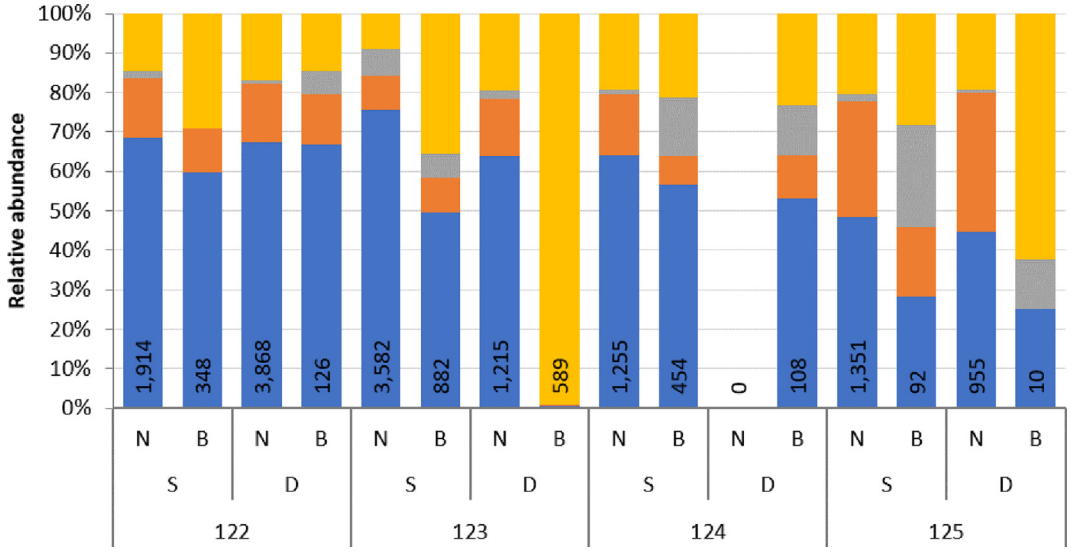

Figure 6. Comparison of relative abundances acquired from cell counts of concentrated net-tow samples (N, size fractions 5–20 and 20–180 μm, i.e., N5+N20 from Fig. 5) and un-concentrated Niskin bottle samples (B). S = surface, D = deep chlorophyll maximum. Values at the base of each bar represent the number of phytoplankton cells counted in each sample. Net-tow samples from TARA_124-D were not available for counting.

pennates' were attributed to either *Pseudo-nitzschia* or *Fragilariopsis* based on the RA of these taxa in the LM dataset. After these manipulations, the two datasets showed a comparable composition (Fig. 8).

Discussion

The present study provides a detailed description of the phytoplankton community composition from four sites around the Marquesas Islands, including a species list, absolute and relative abundances based on several different microscopic techniques, comparison with 18S rRNA metabarcoding data, and characterization of phytoplankton community variation using an ordination method.

The Marquesas Islands are surrounded by oligotrophic waters of the southern subtropical Pacific Ocean. A combination of several environmental factors, also known as the island mass effect, cause perennial higher primary productivity westward from the islands (Signorini et al. 1999; Legeckis et al. 2004; Martinez & Maamaatuaiahutapu 2004). With respect to phytoplankton composition, the study area is one of the least investigated areas in the global ocean, with only a handful of qualitative (Rampi 1952; Hasle 1960) or quantitative studies (Hasle, 1959; Gomez et al. 2007) conducted in the tropical Central Pacific. Our findings show generally low cell abundances in the collected samples, which are comparable to or higher than the surrounding phytoplankton-poor equatorial oceanic waters (Iriarte and Fryxell, 1992), but lower than those found in the Marquesas area during the Biosope expedition in late October (3.1×10^4 cells L^{-1}) (Gomez et al. 2007) or north of the equator and about 6,000 km north of our sampling area in March (up to 7.0×10^4 cells L^{-1}) (Hasle, 1959). However, it is not possible to judge whether these differences result from spatial or temporal differences among these sampling cruises. In spite of the documented lower cell densities matching the very low chlorophyll values, it is clear that TARA_123 and the surface layer of TARA_124 showed higher phytoplankton densities as compared to the pre-algal-bloom (TARA_122) and post-algal-bloom (TARA_125) stations (Fig. 4).

Our results show diatoms dominating the cell counts, despite being represented by a smaller number of species compared to dinoflagellates. Another large-scale study, the Malaspina-2010 expedition, reported a diatom/dinoflagellate cell abundance ratio of 2.5 from the subtropical oligotrophic ocean (Estrada et al. 2016), i.e., around two times lower than in our study (mean 5.7). Based on collections at 145 oceanic stations during that expedition from the Atlantic, Indian and Pacific Oceans, the contribution of diatoms was only important in regions with shallow nutriclines

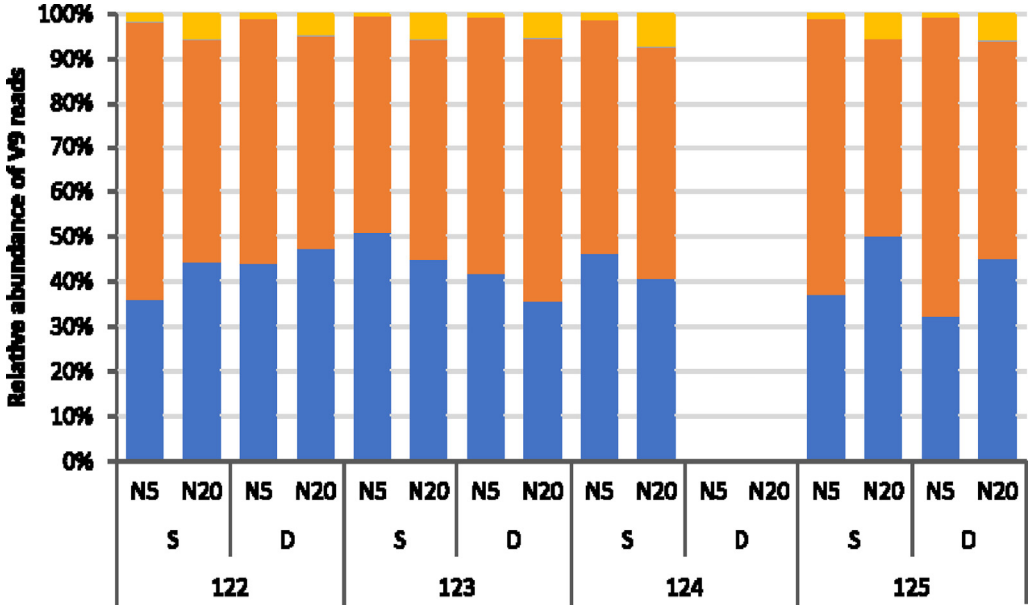

Figure 7. Relative abundances of phytoplankton V9 reads, size fractions of 5–20 μm (N5) and 20–180 μm (N20). S = surface, D = deep chlorophyll maximum. Color coding of the phyla is equal to Fig. 4. Sample TARA_124 D was not available in either size fraction for enumeration.

(i.e., nutrient-rich layers near the surface), such as the equatorial upwelling regions. This seems to be similar to the case of the algal bloom in the vicinity of the Marquesas Islands, where diatoms apparently also play a key role.

Regarding the species composition of phytoplankton around the Marquesas Islands, the proportion among groups differed from that observed in cell abundance data. The most species-rich taxonomic groups turned out to be dinoflagellates, representing 60% of the total 289 documented phytoplankton taxa, followed by diatoms accounting for 32%. A similar proportion between the number of dinoflagellate and diatom species was described in samples from nutrient-enriched and likely more polluted Black Sea environments, where microscopic examination revealed 71 species consisting of 58% of dinoflagellates, 25% of diatoms, and 17% of members of other groups (Agirbas et al. 2017). The limited representation of the other phytoplankton groups is largely influenced by the fact that microscopy methods mainly address the diversity of groups having distinct morphological features even in fixed samples, while all the groups mainly consisting of tiny and naked cells require specific identification techniques. Interestingly, several species previously found to be dominant or widespread in the subtropical and equatorial Central

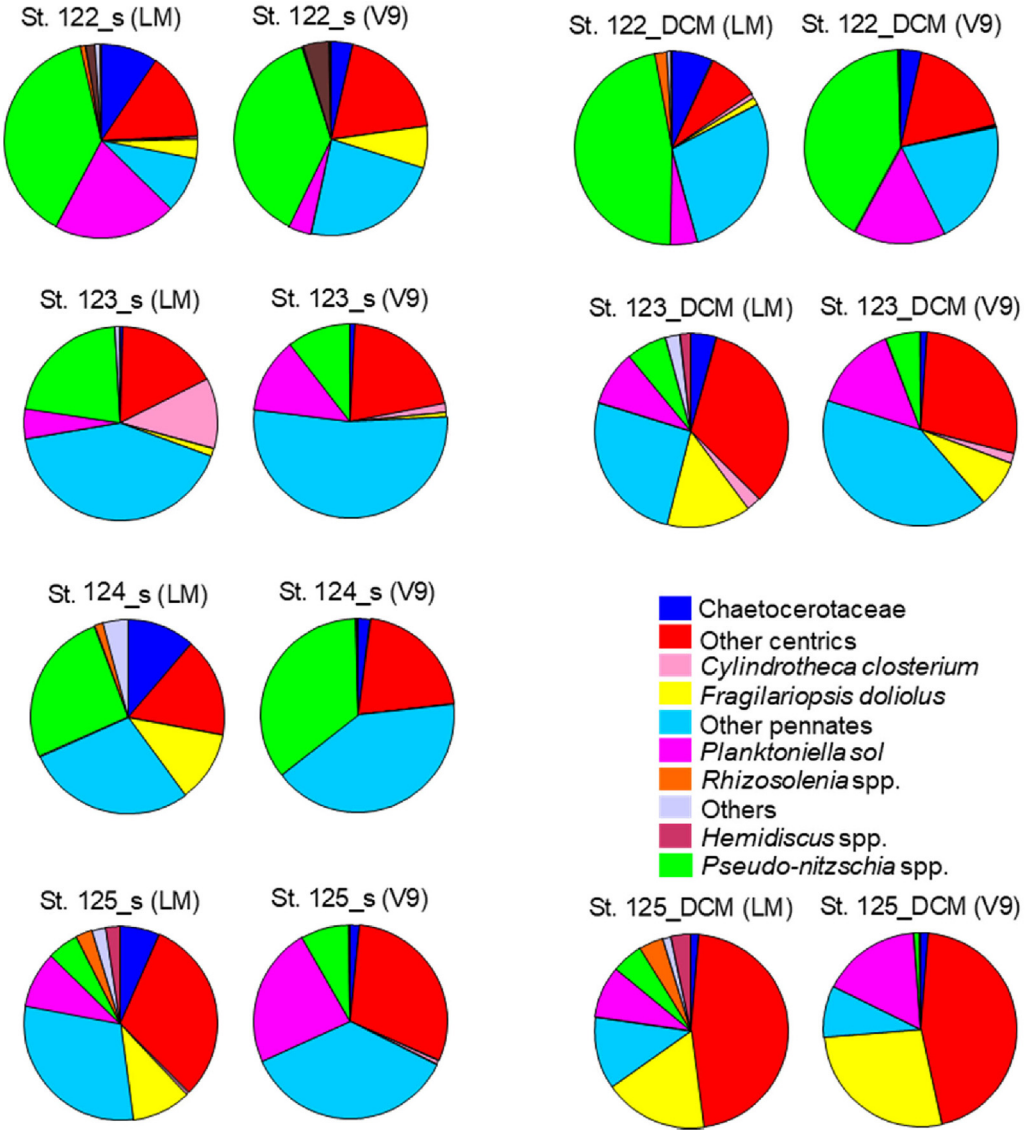

Figure 8. Comparison between the relative abundance of diatoms in light microscopy counts (LM) and metabarcodes (V9) in the 20-180 μm size-fraction.

Pacific, namely the diatoms *Pseudo-nitzschia* cf. *delicatissima*, *Planktoniella sol* and *Rhizosolenia bergoni*, and the dinoflagellates *Oxytoxum variabile, Histioneis* spp. and *Tripos* spp. (Hasle 1960; Gomez et al. 2007), are the same as those found in our study. Such a correlation indicates relatively stable species associations in this area across the seasons, despite the paucity of information. However, the list of species found in the present investigation at four sites is longer than those previously reported for the tropical Central Pacific. For example, Rampi (1952) documented 210 species (170 dinoflagellates, including varieties and forms) and 40 diatoms from a considerably wider equatorial area. In the same study, *Planktoniella sol* was seen to be attached to the tintinnid *Eutintinnus lusus undae* (Rampi 1952). We did not note any of these associations, nor that between tintinnids and *Chaetoceros daday*, also reported by Rampi (1952), nor between *Fragilariopsis doliolus* and other tintinnids seen in the *Tara* Oceans samples from the south Atlantic Ocean (Vincent et al. 2018), although partner species of these associations were present in our samples.

In terms of diversity, it is necessary to keep in mind that the sample volume used can predetermine the outcome of its assessment. Cermeño et al. (2013) pointed out that although microorganisms usually attain high population densities, it should not be assumed that the observation of samples of a few tens of millilitres suffices to completely characterize the species assemblage. It was furthermore shown that marine phytoplankton communities have been particularly under-sampled in ecosystems of low productivity (Cermeño et al. 2013), thus leading to biases in the patterns of previously reported diversity. This is a serious problem. Because our samples originated from a region with generally low productivity, we used multiple techniques (LM, eHCFM and SEM), large volumes, and sometimes several replicates of the same sample to maximize the number of encountered species. Thus, despite the observed low cell densities, the obtained species richness was much higher compared to similar studies. However, species richness and its changes should not be considered alone, as environmental changes may affect ecosystem functions without altering species richness, most notably by affecting population densities and community composition (Spaak et al. 2017). Indeed, species richness is just a single variable reflecting the state of the environment. Therefore, both cell densities and detailed community composition should be taken into account.

The applied ordination methods shed some light on the variation in community composition, and the community response to several environmental characteristics. Unfortunately, the deep sample from TARA_124 was not available for most counts, and was thus excluded from the statistical analyses, decreasing the already small number of counts available for testing and diminishing the robustness of the tests. Based on the results from PCA, diatoms and coccolithophores showed a preference, albeit not significant, for surface layers, whereas dinoflagellates and other groups tended to be prevalent in deeper waters.

Surprisingly, there is still very little information available about the species composition of marine phytoplankton, especially when one realizes how key the role of this organismal assemblage is for the wellbeing of our planet. Fortunately, within the last few years the situation has improved thanks to high throughput analyses of large datasets collected by global oceanic expeditions (Karsenti et al. 2011; Duarte 2015; Sunagawa et al. 2020). The abundances of individual protist groups were mostly derived from the V9 and/or V4 metabarcodes of the 18S rRNA (Massana et al. 2015; Le Bescot et al. 2016; Malviya et al. 2016; Flegontova et al. 2018; Flegontova et al. 2023), and since billions of these sequences from thousands of samples have been analyzed, a general picture is slowly emerging. While in most aspects the molecular data are in good agreement with other methods, typically from microscopy-based analyses of phytoplankton (de Vargas et al. 2015), there are also significant incongruences. A prominent example is that of diplonemids, a group of euglenozoan protists which was until very recently not encountered by light and electron microscopy. However, their dominant presence in V9-based datasets (Flegontova et al. 2018; Flegontova et al. 2023) has now been confirmed by other molecular approaches (Tashyreva et al., 2022).

A direct comparison between datasets obtained with optical methods and metabarcoding surveys is hard to achieve yet very important (Karlusich et al. 2022). At high taxonomic level, the group for which microscopy and molecular data are less coherent is represented by Dinophyceae. This is not unexpected, since organisms belonging to this group possess large genomes with multiple copies of 18S rRNA genes (Prokopowich et al., 2003; Gong & Marchetti 2019), which leads to an overes-

timation of Dinophyceae by molecular approaches. Conversely, Bacillariophyta show the best correlation and similarity between the different approaches. At lower taxonomic level the comparison is even harder, especially for poorly known areas of the global ocean, because the molecular and morphological approaches have different resolution powers for both identification and detection. A first limitation stems from the scarce availability of reference sequences for tropical oceanic species, which have rarely been cultivated and characterized molecularly. This bias prevents the identification of a high number of sequences from the environment. In the case of the *Tara* Oceans samples from the Central Pacific analyzed in our study, more than 60% of the diatom reads could not be attributed to any known genus (Malviya et al. 2016).

From the diversity point of view, the molecular dataset has a higher detection power and hence includes a higher number of less abundant or rare taxa that are hardly found in the small seawater volumes that are generally observed in microscopy analyses. Moreover, many naked forms of dinoflagellates and small flagellates, which often represent the most abundant protists in oligotrophic areas, cannot be identified in fixed samples used for light microscopy. On the other hand, in many cases molecular tags cannot be assigned to known species, while the optical methods allow assignments to many taxa that have only been described based on morphology. A comparison is possible only for diatoms, which are identified relatively well both in microscopy and molecular data, but even in this case the data need to be interpreted taking into account the limitations of both approaches. For example, whole diatom genera such as *Asterolampra*, *Asteromphalus* and *Hemidiscus* are completely missing from the reference dataset of the V9 fragment which, in addition, often lacks the adequate resolution to distinguish between closely related genera, such as *Chaetoceros* and *Bacteriastrum*, and *Thalassiosira* and *Shionodiscus*. In the case of the present data, the comparison worked relatively well for microplankton samples (20-180 μm) of diatom taxa identifiable both via LM and their molecular signatures. These included the Chaetocerotaceae *Chaetoceros* and *Bacteriastrum* and *Planktoniella sol*, as well as *Pseudo-nitzschia* species and *Fragilariopsis doliolus,* which showed similar relative abundance patterns across samples, once the results between the morphological and molecular data were adequately lumped and interpreted. This quite good match, also observed in other diatom studies (Malviya et al. 2016; Piredda et al., 2018), suggests that microscopic and genetic approaches can be highly compatible, reinforcing the idea that rich and curated reference databases and well-defined diagnostic characters are both crucial for reconciliation of molecular and morphology-based taxonomy. Hence, it is obvious that both molecular- and morphology-based methods need to be used in the study of planktonic protists, as they are, despite significant differences, complementary. Consequently, only their combination will eventually lead to the emergence of a robust, complex and stable view of the composition of oceanic plankton (Karlusich et al. 2022).

To some, microscopic examinations might seem as a coarse and insufficient tool for the description of phytoplankton assemblages. The method may indeed be inadequate for the characterization of picoplankton cells, as observed by Estrada et al. (2016), or of those falling in the size fraction 0.8–5 μm as in our study. However, although tedious, time consuming and requiring the increasingly scarce taxonomic expertise, microscopy remains irreplaceable. With the flood of molecular data, we predict that it will actually be increasingly important for matching them with morphological properties. While the results on group composition obtained from molecular data largely matched those obtained with morphological methods, the latter allowed us to dissect species composition in detail and to assess environmental preferences of taxonomic groups, highlighting the complementarity of the two approaches. The morphological methods can be particularly informative in remote areas, where the number of unassigned environmental sequences is higher because of the prevalence of uncultivated species that are not represented in reference datasets. This approach allowed us to dissect species composition in detail and to assess environmental preferences of taxonomical groups. We believe that the present study illuminates a fraction of the marine phytoplankton flora from around the Marquesas Islands and provides a small but solid base for future ecological and biogeographical studies of global marine biota.

CRediT authorship contribution statement

Jana Veselá-Strejcová: Conceptualization, Methodology, Software, Visualization, Investigation. **Eleonora Scalco:** Visualization, Investigation.

Adriana Zingone: Data curation, Writing – original draft. **Sébastien Colin:** Data curation, Writing – original draft. **Luigi Caputi:** Data curation, Writing – original draft. **Diana Sarno:** Visualization, Investigation. **Jana Nebesářová:** Visualization, Investigation. **Chris Bowler:** Data curation, Writing – original draft. **Julius Lukeš:** Data curation, Writing – original draft, Supervision, Writing – review & editing.

Data availability

Data will be made available on request.

Declaration of Competing Interest

The authors declare that they have no known competing financial interests or personal relationships that could have appeared to influence the work reported in this paper.

Acknowledgements

The *Tara* Oceans consortium acknowledges the origin of samples from Stations TARA_122-125 as French Polynesia and that they were collected under Convention number 3534 (Convention relatif à la campagne de prélévements et de mésures de Tara Oceans en Polynesie Francaise) dated 16 June 2011. We thank the commitment of the following people and sponsors who made this singular expedition possible: CNRS (in particular Groupement de Recherche GDR3280, the Mission Pour l'Interdisciplinarité – Project MEGALODOM, and the Fédération de Recherche GO-SEE FR2022), European Molecular Biology Laboratory (EMBL), Genoscope/CEA, the French Government "Investissements d'Avenir" programs Oceanomics (ANR-11-BTBR-0008), MEMO LIFE (ANR-10-LABX-54), PSL* Research University (ANR-11-IDEX-0001-02), and FRANCE GENOMIQUE (ANR-10-INBS-09), EU FP7 (MicroB3/No.287589), ERC Advanced Grant Awards (Diatomite: 294823 and Diatomic: 835067), the LouisD Foundation of the Institut de France, a Radcliffe Institute Fellowship from Harvard University to C. B., agnès b., the Veolia Environment Foundation, Region Bretagne, World Courier, Illumina, Cap L'Orient, the EDF Foundation EDF Diversiterre, FRB, the Prince Albert II de Monaco Foundation, Etienne Bourgois, the Fonds Français pour l'Environnement Mondial, the TARA schooner and its captain and crew. This article is contribution number XXX of *Tara* Oceans. This project was also supported by the ERD Funds 16_019/0000759 and the Czech Science Foundation grant 23-06479X to J.L., and the Czech Bioimaging grant LM2018129 to J.N. E.S. was supported by the Italian RITMARE flagship project, funded by MIUR, approved by the CIPE Resolution 2/2011. We thank Colomban de Vargas and Margaux Carmichael (Biological Station, Roscoff) for providing the samples. Jiří Vaněček, Petra Masařová, Martina Tesařová and Tomáš Bílý (Biology Centre) helped with optimization of protocols and processing of the samples.

Appendix A. Supplementary material

Supplementary data to this article can be found online at https://doi.org/10.1016/j.protis.2023.125965.

References

Abreu A, Bourgois E, Gristwood A, et al. (2022) Priorities for ocean microbiome research. Nat Microbiol **7**:937–947

Adl SM, Bass D, Lane CE, Lukeš J, Schoch CL, et al. (2019) Revision to the classification, nomenclature and diversity of eukaryotes. J Eukaryotic Microbiol **66**:4–119

Agirbas E, Koca L, Aytan U (2017) Spatio-temporal pattern of phytoplankton and pigment composition in surface waters of south-eastern Black Sea. Oceanologia **59**:283–299

Aumont O, Ethé C, Tagliabue A, Bopp L, Gehlen M (2015) PISCES-v2: an ocean biogeochemical model for carbon and ecosystem studies. Geosci Model Dev **8**:2465–2513

Bengtson P (1988) Open nomenclature. Palaeontology **31**:223–227

Berney C, Ciuprina A, Bender S, Brodie J, Edgcomb V, et al. (2017) UniEuk: Time to speak a common language in Protistology! J Eukaryot Microbiol **64**:407–411

Bowler C (2013) Tara Oceans: Comprehensive biogeographic insights into the complexity of marine diatom communities. Phycologia **52(Suppl)**:12

Caputi L, Carradec Q, Eveillard D, et al. (2019) Community-level responses to iron availability in open ocean planktonic ecosystems. Global Biogeochem Cycles **33**:391–419

Carbonell-Moore MC (2017) The rediscovery of *Archaeosphaerodiniopsis* Rampi (Dinophyceae). Eur J Phycol **52**:57–63

Caron DA, Countway PD, Jones AC, Kim DY, Schnetzer A (2012) Marine protistan diversity. Ann Rev Mar Sci **4**:467–493

Cermeño P, Rodríguez-Ramos T, Dornelas M, et al. (2013) Species richness in marine phytoplankton communities is not correlated to ecosystem productivity. Mar Ecol Prog Ser **488**:1–9

Colin S, Coelho LP, Sunagawa S, Bowler C, Karsenti E, Bork P, Pepperkok R, de Vargas C (2017) Quantitative 3D-imaging for cell biology and ecology of environmental microbial eukaryotes. Elife **6**:e26066

Colin S (2022) Taxonomic annotations of confocal microscopy images of environmental protists from the Marquesas Islands (Tara Oceans survey, Southern Pacific Ocean). BioStudies 2022:S-BIAD595. https://www.ebi.ac.uk/biostudies/BioImages/studies/S-BIAD595

Cupp EE (1943) Marine plankton diatoms of the west coast of North America. Bull Scripps Inst Oceanogr **5**:1–237

de Vargas C, Audic S, Henry N, et al. (2015) Eukaryotic plankton diversity in the sunlit ocean. Science **348**:1261605

Dodge JD (1982) Marine dinoflagellates of the British Isles. Her Majesty's Stationary Office; London

Duarte CM (2015) Seafaring in the 21st Century: The Malaspina 2010 Circumnavigation Expedition. Limnol Oceanogr Bull **24**:11–14

Ducklow DK, Steinberg KO, Buesseler KO (2001) Upper ocean carbon export and the biological pump. Oceanography **14(4)**:50–58

Estrada M, Delgado M, Blasco D, et al. (2016) Phytoplankton across tropical and subtropical regions of the Atlantic, Indian and Pacific Oceans. PLoS ONE **11**:e0151699

Field CB, Behrenfield MJ, Randerson JT, Falkowski P (1998) Primary production of the biosphere: Integrating terrestrial and oceanic components. Science **281**:5374

Flegontova O, Flegontov P, Malviya S, Poulain J, de Vargas C, Bowler C, Lukeš J, Horák A (2018) Neobodonids are dominant kinetoplastids in the global ocean. Environ Microbiol **20**:878–889

Flegontova O, Flegontov P, Jachníková N, Lukeš J, Horák A (2023) Water masses shape pico-nano eukaryotic communities of the Weddell Sea. Communications Biology **664**

Gómez F, Claustre H, Raimbault P, Souissi S (2007) Two high-nutrient low-chlorophyll phytoplankton assemblages: the tropical central Pacific and the offshore Peru-Chile Current. Biogeosciences **4**:1101–11013

Gong W, Marchetti A (2019) Estimation of 18S gene copy number in marine eukaryotic plankton using a next-generation sequencing approach. Front Mar Sci **6**. https://doi.org/10.3389/fmars.2019.00219

Grob C, Ulloa O, Claustre H, Huot Y, Alarcón G, Marie D (2007) Contribution of picoplankton to the total particulate organic carbon concentration in the eastern South Pacific. Biogeosciences **4**:837–852

Hasle GR (1959) A quantitative study of phytoplankton from the equatorial Pacific. Deep Sea Research **6**:38–59

Hasle GR (1960) Phytoplankton and ciliate species from the tropical Pacific. Skr Norske Vidensk - Akad Oslo, Mat Naturvidens Kl **2**:1–50

Iriarte JL, Fryxell GA (1992) Micro-phytoplankton at the equatorial Pacific during the JGOFS EqPac Time Series studies: March to April and October 1992. Deep-Sea Res II **42**:559–583

Karlusich JJP, Lombard F, Irisson J-O, Bowler C, Foster RA (2022) Coupling imaging and omics in plankton surveys: State-of-the-art, challenges, and future directions. Front Mar Sci **9**:878803

Karsenti E, Acinas SG, Bork P, et al. (2011) A holistic approach to marine eco-systems biology. PLoS Biol **9**: e1001177

Le Bescot N, Mahé F, Audic S, Dimier C, Garet M-J, Poulain J, Wincker P, de Vargas C, Siano R (2016) Global patterns of pelagic dinoflagellate diversity across protest size classes unveiled by metabarcoding. Environ Microbiol **18**:609–626

Legeckis R (1977) Long waves in the eastern equatorial Pacific Ocean: A view from a geostationary satellite. Science **197**:1179–1181

Legeckis R, Brown CW, Bonjean F, Johnson ES (2004) Influence of tropical instability waves on phytoplankton blooms in the wake of the Marquesas Islands during 1998 and on the currents observed during the drift of the Kon-Tiki in 1947. Geophys Res Lett **31**:L23307

Malviya S, Scalco E, Audic S, et al. (2016) Insights into global diatom distribution and diversity in the world's ocean. Proc Nat Acad Sci USA **113**:E1516–E1525

Martinez E, Maamaatuaiahutapu K (2004) Island mass effect in the Marquesas Islands: Time variation. Geophys Res Lett **31**:1–4

Masquelier S, Vaulot D (2008) Distribution of micro-organisms along a transect in the South-East Pacific Ocean (BIOSOPE cruise) using epifluorescence microscopy. Biogeosciences **5**:311–321

Massana R, Gobet A, Audic S, Bass D, Bittner L, et al. (2015) Marine protist diversity in European coastal waters and sediments as revealed by high-throughput sequencing. Environ Microbiol **17**:4035–4049

Oksanen J, Kindt R, Legendre P, O'Hara B, Stevens MHH, Oksanen MJ, Suggests MASS (2007) The vegan package. Community Ecol Package **10**:719

Pesant S, Not F, Picheral M, et al. (2015) Open science resources for the discovery and analysis of Tara Oceans data. Sci Data **2**:150023

Picheral M., Colin S., Irisson J.-O. (2017) EcoTaxa, a tool for the taxonomic classification of images. Available from: http://ecotaxa.obs-vlfr.fr.

Piredda R, Claverie J-M, Decelle J, et al. (2018) Diatom diversity through HTS-metabarcoding in coastal European seas. Sci Rep **8**:18059

Prokopowich CD, Gregory TR, Crease TJ (2003) The correlation between rDNA copy number and genome size in eukaryotes. Genome **46**:48–50

Queguiner B (2013) Iron fertilization and the structure of planktonic communities in high nutrient regions of the Southern Ocean. Deep Sea Res Part II **90**:43–54

Rampi L (1943) Su qualche altra Peridinea nuova o rara delle acque di Sanremo. Atti della Società Italiana di Scienze Naturali e del Museo civico di Storia Naturale in Milano **82 (2)**:151–157

Rampi L (1952) Ricerche sul Microplancton di superficie del Pacifico tropicale. Bull Institut Oceanogr Monaco **1014**:1–16

Rampi L, Bernard M (1980) Chiave per la determinazione delle peridinee pelagiche mediterranee. Comitato Nazionale Energia Nucleare **5**:1–193

Sigman DM, Hain MP (2012) The Biological productivity of the ocean. Nat Educ Knowledge **3**:21

Signorini SR, McClain CR, Dandonneau Y (1999) Mixing and phytoplankton bloom in the wake of the Marquesas Islands. Geophys Res Lett **26**:3121–3124

Smetacek V, Naqvi SWA (2008) The next generation of iron fertilization experiments in the Southern Ocean. Phil Trans R Soc A **366**:3947–3967

Spaak JW, Baert JM, Baird DJ, et al. (2017) Shifts of community composition and population density substantially affect ecosystem function despite invariant richness. Ecol Lett **20**:1315–1324

Sunagawa S, Acinas SG, Bork P, et al. (2020) Tara Oceans: towards global ocean ecosystems biology. Nat Rev Microbiol **18**:428–445

Tashyreva D, Simpson A, Prokopchuk G, et al. (2022) Diplonemids – a review on „new" flagellates on-the-oceanic-block. Protist **173**:125868

Thomas CR (1997) Identifying marine phytoplankton. Academic Press; San Diego

Utermöhl H. (1958) Zur der Vollkommung der quantitativen Phytoplankton-methodik. *Mitteilung Internationale Vereinigung Fuer Theoretische und Angewandte Limnologie*, 9, 39 pp.

Vincent FJ, Colin S, Romac S, et al. (2018) The epibiotic life of the cosmopolitan diatom *Fragilariopsis doliolus* on heterotrophic ciliates in the open ocean. ISME J **12**:1094

Worden AZ, Follows MJ, Giovannoni SJ, et al. (2015) Rethinking the marine carbon cycle: Factoring in the multifarious lifestyles of microbes. Science **347**:1257594

Zingone A, Harrison PJ, Kraberg A, et al. (2015) Increasing the quality, comparability and accessibility of phytoplankton species composition time-series data. Estuar Coast Shelf Sci **162**:151–160

Zingone A, Veselá J, Nebesářová J, Scalco E, Sarno D, Lukeš J, Colin S (2022) A large collection of scanning electron microscopy images of protists and their taxonomic annotations from the Marquesas Island area (Tara Oceans survey, Southern Pacific Ocean). BioStudies 2022:S-BIAD598. https://www.ebi.ac.uk/biostudies/bioimages/studies/S-BIAD598